Modeling Impacts of Nutrient Loading, Warming, and Boundary Exchanges on Hypoxia and Metabolism in a Shallow Estuarine Ecosystem

Jeremy M. Testa (iD), *Nicole Basenback, Chunqi Shen, Kelly Cole, Amanda Moore, Casey Hodgkins, and Damian C. Brady*

Research Impact Statement: Future warming will decrease net ecosystem metabolism and increase hypoxia in a small estuary, but warming and nutrient load effects on connected waterbodies will also be translated into the estuary.

ABSTRACT: We sought to investigate the impacts of nutrient loading, warming, and open-water boundary exchanges on a shallow estuary through idealized numerical model experiments. We performed these simulations using a stand-alone implementation of the Regional Ocean Modeling System-Row-Column AESOP biogeochemical model in the Chester River estuary, a tributary estuary within the Chesapeake Bay estuarine complex. We found that metabolic rates were elevated in the shallow tributary creeks of the estuary relative to open waters and that rates of gross primary production, respiration, and net ecosystem metabolism were a function of both water temperature and local phytoplankton biomass. Warming 0.75°C and 1.25°C led to reductions in dissolved oxygen concentrations throughout the estuary. Reductions (50%) in dissolved nitrogen and phosphorus loading did not substantially alter hypoxic volumes in this turbid, nutrient-rich estuary, but warming increased hypoxic volumes by 20%–30%. Alterations of the open-water boundary that represent improved oxygen concentrations in the adjacent Chesapeake Bay mainstem led to more substantial relief of hypoxia in model simulations than nutrient reductions (~50% reductions in hypoxia). These simulations reveal the complex interplay of watershed nutrient inputs and horizontal exchange in a small tributary estuary, including the finding that future warming and nutrient reduction effects on Chesapeake Bay hypoxia will be translated to some tributary estuaries like the Chester River.

(KEYWORDS: eutrophication < ECOLOGY; total maximum daily loading (TMDL) < WATER QUALITY; estuaries < GEOGRAPHY; Chesapeake Bay; Chester River estuary; climate variability/change < CLIMATE; metabolism; biogeochemical model.)

INTRODUCTION

Biogeochemical processes in coastal ecosystems are closely linked to adjacent land use, internal physical, biological, and chemical processes, and remote forcing from adjacent tidal waters. A key interaction within the Anthropocene is the alteration of watershed nutrient budgets and hydrology through urbanization and agricultural expansion and intensity combined with warming temperature and altered precipitation patterns. Elevated nutrient loading combined with warmer, wetter conditions in many temperate ecosystems is associated with enhanced oxygen depletion

(Laurent et al. 2018; Ni et al. 2019), altered phytoplankton biomass (Boynton et al. 1982), and pressures on macrophyte and benthic communities (Lefcheck et al. 2017). While the potential scope of biogeochemical changes associated with eutrophication and climate change is large, it remains a challenge to meaningfully predict future changes given uncertainties in projected climate variability, the effects of climate on phytoplankton production and composition, and watershed dynamics (Wagena et al. 2018). This is especially true considering that climate will impart differential impacts on components of coupled human-watershed-estuarine systems via changes in hydrology (Neff et al. 2000), temperature (Altieri and Gedan 2015), solar radiation (Nixon et al. 2009), and agricultural practices (Ortiz-Bobea et al. 2019).

Due to the nature of their bathymetry and proximity to land, shallow estuarine systems have several unique characteristics compared to larger, deeper systems. Whereas deep estuaries have production and respiration cycles dominated by water-column plankton (e.g., Fennel and Testa 2019), shallow estuaries can be dominated by benthic metabolism from submerged aquatic vegetation (Ganju et al. 2020), microphytobenthos (McGlathery et al. 2007), or subtidal sediments. One consequence of this distinction is that oxygen depletion in deeper systems tends to be a seasonal, kilometer-scale phenomenon supported by sinking phytoplankton-derived organic material, whereas shallow ecosystems can generate local diel cycling hypoxia over 6–12 h as a result of high rates of benthic metabolism or high rates of water-column respiration associated with high phytoplankton biomass (>100 µg/L; e.g., Tyler et al. 2009). In the case of the Chesapeake Bay and other drowned river valleys, shallow tributary estuaries are also responsive to the influence of larger, adjacent water bodies where water exchange can lead to import of organic material (Smith et al. 1991), high-nutrient or low-oxygen water into their lower reaches on seasonal or event scales (L. P. Sanford and Boicourt 1990; Testa et al. 2008), or poorly buffered upwelling water (Grantham et al. 2004).

Numerical models have been widely used to generate projections of future conditions in response to climate warming, precipitation (and freshwater input) changes, and nutrient abatement actions (Meier et al. 2011; Irby et al. 2018; Lajaunie-Salla et al. 2018; Laurent et al. 2018; Ni et al. 2019). The rationale for using complex, three-dimensional numerical models to generate future projections is that they integrate the coupled biogeochemical–hydrodynamic interactions that will result from altered physical and chemical conditions.

In particular, simulations quantify how climate changes (e.g., warming, elevated river flow) may make the achievement of water quality standards more difficult, resulting in adjusted allocations for nutrient reduction targets (Justić et al. 2003; Irby et al. 2018). In general, these projections have been made for large, relatively deep coastal ecosystems where sophisticated numerical models had previously been developed (e.g., northern Gulf of Mexico, Baltic Sea, Chesapeake Bay, Salish Sea). Far fewer model projections have been made for very shallow coastal systems that fringe the land–sea interface (Lajaunie-Salla et al. 2018), despite the fact that these shallow ecosystems are (1) likely to be highly sensitive to future climatic change, (2) locations if intense biogeochemical processing of watershed inputs, and (3) important areas for tourism, fisheries, and aquaculture.

The purpose of this paper was to use a three-dimensional coupled hydrodynamic-biogeochemical model to quantify the sensitivity of oxygen depletion and metabolism in a shallow estuary to elevated temperature, altered nutrient inputs, and oxygen conditions at the open-water boundary. We use the Chester River estuary as an experimental system, as it includes both seasonal, deep water hypoxia, and shallow water diel cycling hypoxia. We present sensitivity simulations over an annual cycle in the estuary, and address the spatial and temporal changes in hypoxia and the metabolic rate processes driving oxygen production and consumption.

METHODS

To evaluate the sensitivity of low oxygen conditions in the Chester River estuary to altered external forcing, we conducted a series of idealized simulations using a coupled, three-dimensional hydrodynamic-biogeochemical model (Regional Ocean Modeling System-Row-Column AESOP [ROMS-RCA]). After validating the model with the best available data, we adjusted three main inputs to the model: (1) nutrient loading from 12 major freshwater sources, (2) factors related to warming from climate projections, and (3) oxygen conditions at the open-water boundary associated with potential changes in hypoxia in the mainstem of the Chesapeake Bay. We did not investigate the impacts of sea level rise or altered precipitation patterns, which are also expected to change in a future climate (Ni et al. 2019). Model response metrics we quantified included ecosystem responses in terms of the volume, duration, and extent of hypoxic waters and

rates of oxygen production and consumption in the water column and sediments.

Study Site

The Chester River estuary is located on the eastern shore of Maryland, a peninsula on the eastern fringe of the Chesapeake Bay (Figure 1). The estuary has a maximum depth of approximately 18 m in a deep channel in the lower estuary, but a majority of the estuary is <6 m deep (Figure 1), especially in several subtributaries (e.g., Corsica River, Langford Creek, Southeast Creek; Figure 2). The 1,140 km^2 watershed consists of predominantly agricultural land use (65%) and lies within the coastal plain. The estuary exchanges with the mainstem of the Chesapeake Bay at its seaward open-water boundary and with Eastern Bay to the

south through a narrow channel at Kent Narrows (Figure 2).

Numerical Model and Data Sources

A coupled hydrodynamic-biogeochemical model was applied to simulate and analyze estuarine biogeochemical responses to simulated changes in nutrient input, temperature, and open-water boundary conditions. The hydrodynamic model is an application of the ROMS with a 174 × 174 grid that includes 200 m horizontal resolution and 10 vertical layers and is a stand-alone implementation that is not nested in a larger domain. Freshwater inputs to the estuary were delivered from 12 major rivers and creeks (Figure 1; Figures S1 and S2) and derived from predictions from the Hydrologic Simulation Program Fortran as part of the Phase 6 Chesapeake Bay Program (CBP)
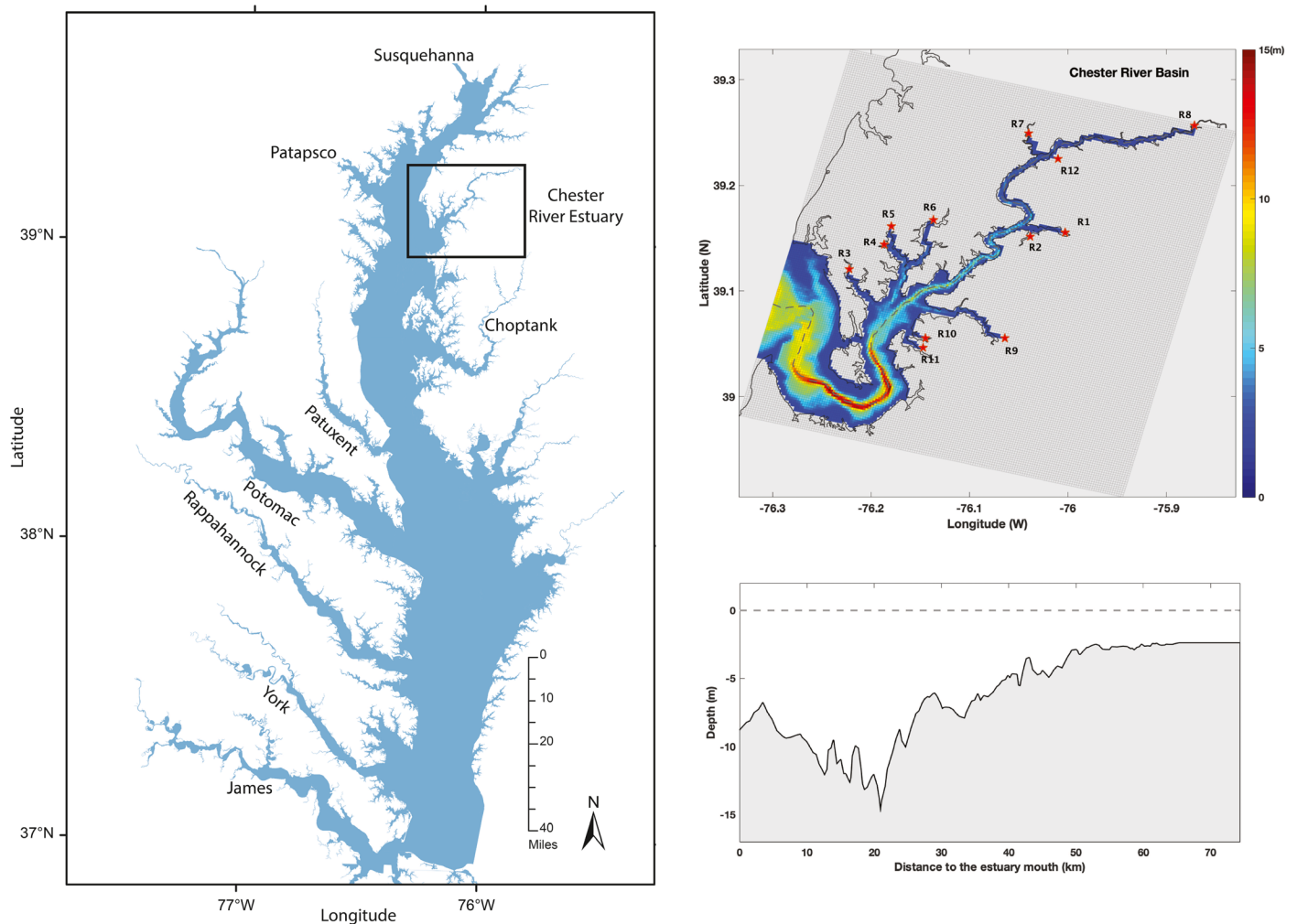

FIGURE 1. Location of the Chester River estuary on the northeastern shore of the Chesapeake Bay (left panel), bathymetry of the Chester River estuary with grid location and freshwater sources (top right panel), and maximum depth distribution along the central channel of the Chester River within the model domain.
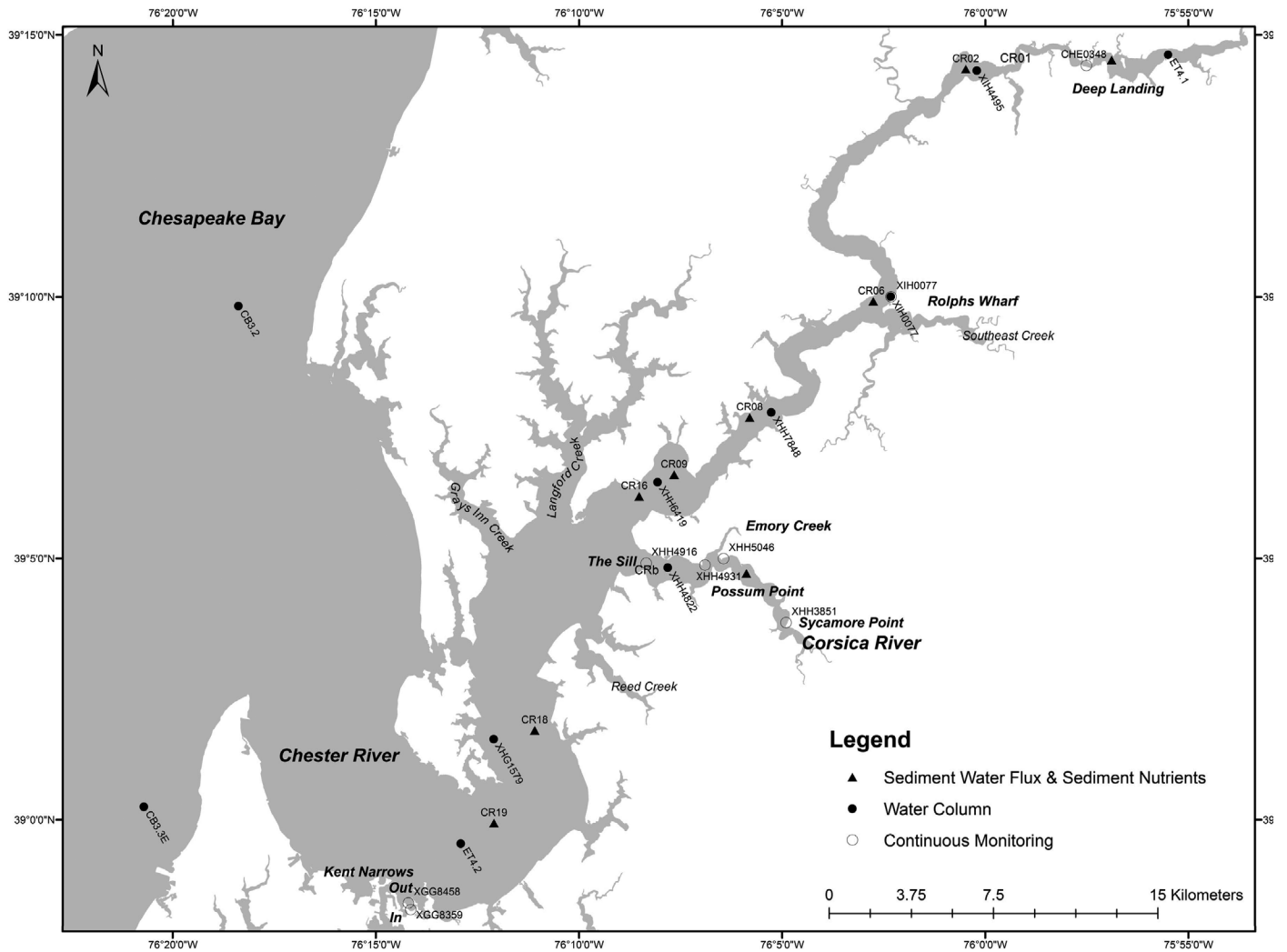
FIGURE 2. Map of water-column and sediment process and concentration measurement and monitoring stations in the Chester River estuary. See Table 1 for station location and measurement types. These include sediment-water flux and sediment nutrients content (triangles) stations, the Chesapeake Bay Program long-term water quality monitoring stations (ET4.1 and ET4.2; closed circles), continuous sensor deployment stations (open circles), and short-term biogeochemical monitoring stations (closed circles).

Watershed Model (Shenk et al. 2012). Atmospheric forcing for net heat flux, total downward radiation, precipitation, and evaporation was derived from the North American Regional Reanalysis (NARR; https://www.ncdc.noaa.gov/data-access/model-data/model-datasets/north-american-regional-reanalysis-narr) product. Wind forcing, air temperature, and barometric pressure were obtained from the Thomas Point buoy located near the Chester River (38.899 N, 76.436 W) and accessed from the National Data Buoy Center (http://www.ndbc.noaa.gov/station_page.php?station=tplm2). Open-water boundary conditions for salinity and water temperature were averaged from two stations in the mainstem Chesapeake Bay (CB3.2 and CB3.3E) monitored on a biweekly to monthly basis (Figure 2). Sea level changes at the open-water boundary were obtained from the CBP Water Quality

and Sediment Transport model (Cerco and Noel 2013). A quadratic stress is exerted at the bed, assuming that the bottom boundary layer is logarithmic over a roughness height of 1 mm.

ROMS was coupled to a biogeochemical model (RCA) that has been described in detail in prior publications (Testa et al. 2014; Ni et al. 2019; Shen, Testa, Li, et al. 2019). In short, RCA models state variables representing at least two phytoplankton groups (representing diatoms and dinoflagellates), labile and refractory pools of dissolved and particulate carbon, nitrogen, phosphorus, and silica, dissolved oxygen (hereafter O_2), and O_2-consuming reduced solutes (CH_4, H_2S). RCA also includes a two-layer sediment module that includes an aerobic and anaerobic layer and represents deposition, remineralization, solute-sediment partitioning, burial, mixing,

and biogeochemical reactions, such as sulfide and ammonium oxidation, and denitrification (Di Toro 2001; Brady et al. 2013; Testa et al. 2013). Initial conditions for water-column state variables were first derived from long-term monitoring stations (Figure 2) and initial sediment conditions were extracted from ROMS-RCA simulations (dissolved constituents) previously simulated for the Chesapeake Bay (Testa et al. 2014; Shen, Testa, Li, et al. 2019) and particulate carbon, nitrogen, and phosphorus content from observations made in 2001 (Frank et al. 2002). The model was then run for an annual cycle to allow for water-column and nutrient conditions to stabilize to locally relevant conditions in the model simulation year 2003. Open-water boundary conditions were derived from the same monitoring stations as for salinity and temperature, and watershed loads of nutrients were derived from the Phase 6 simulation of the Chesapeake Bay Watershed Model.

Model Validation Data

The base 2003 model simulation was validated using bi-monthly to monthly, station-specific measurements of salinity, water temperature, chlorophyll-a, dissolved (DON, DOP, NO_{23}, NH_4, and PO_4) and particulate nutrient concentrations, and O_2 from the CBP monitoring program (https://www.chesapeakebay.net) at several stations in the main estuarine channel (Figure 2) and several additional stations along the shallow shoals (Figure 2). High-frequency data from the Maryland Department of Natural Resources Continuous Monitoring (ConMon) program (http://eyesonthebay.dnr.maryland.gov/) were also used to validate the model, where salinity, temperature, and O_2 were measured. ConMon data are collected via a Xylem/YSI sonde containing multiple sensors sampling water properties (salinity, temperature, and O_2) every 15 min. Sondes are replaced with a newly calibrated instrument every ~two weeks and discrete water samples for chlorophyll-a, total suspended solids (TSS), nutrients, and particulate organic matter were collected at these times to post-calibrate sensors. We also compared simulated rates of sediment-water fluxes of nitrate (NO_{23}), ammonium (NH_4), phosphate (PO_4^-), and O_2 (sediment oxygen demand; SOD) using observations made at several stations during the summer of 2001 (June–August; Figure S5) in intact sediment core incubations in the Chester and Corsica River estuaries (Boynton et al. 2018).

We used multiple model-data comparison metrics to assess the ability of the model to simulate biogeochemical dynamics, including root mean square error (RMSE), mean error (ME), and the reliability index (RI). Complete details and equations for the metrics can be found in Stow et al. (2009) and Fitzpatrick (2009), but in brief, RMSE quantifies the magnitude of overall model-data discrepancies, whereas ME indicates both the magnitude and direction of the mean of model-data discrepancies. Both RMSE and ME are in the same units as the variable of interest. The RI describes the average multiplicative difference between model output and observations. For example, an RI of 2 would indicate that the model predicts the observations within a factor of 2.

Nutrient Reduction Scenarios

We tested the sensitivity of the Chester River O_2 concentrations to changes in the overall magnitude of both nitrate and phosphate loading. Model scenarios consisted of decreasing the nitrogen (NO_{23}, nitrate + nitrite) and phosphorus (PO_4) concentrations in stream discharges for each of the 12 major rivers by 50%, where the decreases were applied uniformly over the annual cycle. NO_{23} and PO_4 reduction scenarios were performed independently, and we did not simulate simultaneous reductions of both nutrients. For comparison, the total Chesapeake Bay total maximum daily load (TMDL) includes a 19.1% reduction in TN and a 23.8% reduction in TP from 2009 loads, whereas the Chester River estuary includes a 17.4% reduction in TN and a 9.8% reduction in TP from 2009 loads (CBP 2010). Here, we hypothesized that nutrient load decreases will generate less extensive and reduced duration hypoxic conditions in main channel bottom waters via reduced phytoplankton production and deposition. We evaluated changes in surface and bottom O_2 concentrations, estuarine volumes of hypoxic water (where hypoxia was defined as <5, 3.2, and 2 mg O_2 L^{-1} using O_2 criteria targets), and the duration of O_2 concentrations less than the three specified O_2 thresholds.

Elevated Temperature Scenarios

We also performed idealized model scenarios of elevated water temperature, where water temperatures were elevated by 0.75°C and 1.25°C in the biogechemical model simulation, applied uniformly to all estuarine cells and on all days within the annual cycle. We did not simulate the hydrodynamic response to temperature by applying warming to the atmospheric, riverine, or open-water boundaries. Recent analyses of the Chesapeake water temperature trends have suggested surface water warming of 0.5°C to >2°C over the past 30 years (Ding and Elmore 2015) and projections of warming suggest increases of at least

1.5°C between the present day and the mid-century (Ni et al. 2019). Given the well-described impacts of water temperature on solubility and metabolic rates (Yvon-Durocher et al. 2012; Breitburg et al. 2018), we quantified the vulnerability of O_2 conditions to future warming. We hypothesized that warming will reduce surface layer O_2 concentrations through reduced solubility, and reduce bottom-water O_2 through elevated respiration and reduced vertical mixing of oxygen.

Sensitivity of Dissolved Oxygen to the Chesapeake Bay Boundary

We simulated a scenario that represents improved oxygen concentrations in the open-water boundary that could be expected from watershed nutrient management in the broader Chesapeake Bay increasing O_2 concentrations at the open-water boundary of the Chester estuary. The lower Chester River estuary exchanges at its open-water boundary with the most severely O_2-depleted region of the Chesapeake Bay (Testa and Kemp 2014), a region that is also vulnerable to future warming-induced hypoxia (Ni et al. 2019). To examine the potential for advection or mixing of Chesapeake Bay bottom waters through the mouth of the Chester River to impact Chester estuary dissolved O_2, we adjusted the open-water O_2 boundary condition to represent reduced hypoxic conditions in Chesapeake Bay. Here, we set bottom O_2 concentrations to those observed in 2001, a year with relatively high O_2 concentrations in the mainstem of the Chesapeake Bay (Li et al. 2016).

Climatic Impacts on Gross Primary Production and Respiration

We used two approaches to assess the potential impacts of climate change on rates of gross primary production (GPP) and respiration. First, we postprocessed the numerical model output to calculate water-column integrated rates of GPP and sediment + water column respiration rates at each hourly time-step. Water-column respiration rates include phytoplankton respiration, organic carbon oxidation, and oxidation of sulfide and methane, whereas sediment respiration rates include the SOD simulated within the sediment flux model module. Comparable approaches to estimating metabolism have been previously applied for ROMS-RCA in the Chesapeake Bay (Testa et al. 2014; Shen, Testa, Ni, et al. 2019).

Second, we estimated ecosystem GPP, respiration, and net ecosystem metabolism (NEM) from observed continuous (15-min) time-series of O_2 at eight locations (Figure 2). The original concept and method for computing gross GPP and respiration (and NEM) was developed in the 1950s (Odum and Hoskin 1958) and has subsequently been modified for a variety of aquatic ecosystems (Caffrey 2004). The approach derives ecosystem rates of GPP (P_g = GPP) and respiration (R_t) from increases in O_2 concentrations during daylight hours and declines during nighttime hours, respectively. The sum of these two processes over 24 h, after correcting for air–sea exchange, provides an estimate of NEM. We used continuous O_2 concentration measurements at eight locations in the Chester River estuary from 2003 to 2016 (Figure 2) to apply a modified approach (Beck et al. 2015), which uses weighted regression to remove tidal effects on O_2 time-series since the tide can advect higher or lower O_2 past the sensor thereby influencing the calculation of NEM. The changes in O_2 used to compute metabolic rates were corrected for air–water gas exchange using the equation $D = K_a (C_s - C)$, where D is the rate of air–water O_2 exchange (mg O_2 L^{-1} h^{-1}), K_a is the volumetric aeration coefficient (h^{-1}), and C_s and C are the O_2 saturation concentration and observed O_2 concentration (mg O_2 L^{-1}), respectively. K_a was computed as a function of wind speed derived from the North American Land Data Assimilation System and details of the air–water gas calculation are incorporated into the R package WtRegDO (Beck et al. 2015) and described in detail elsewhere (Thébault et al. 2008). The calculations utilized salinity, temperature, and O_2 timesseries from the sensors at each platform, and atmospheric pressure and air temperature data from the NARR. Tidal height data were obtained from a nearby NOAA station at Tolchester Beach, Maryland (https://tidesandcurrents.noaa.gov/waterlevels.html?id=8573364). The O_2 data used to make metabolic computations were obtained from sensors deployed near-bottom in relatively shallow waters (Table 1) that were well-mixed, which is necessary for the air–water flux correction to be valid and for the O_2 time-series to be representative of the combined water column and sediments (Murrell et al. 2018).

RESULTS

We present a validation of baseline biogeochemical model simulation against observed concentrations and metabolic rates for key conditions in 2003, a year with consistently high freshwater input (Figure 3). The seasonal cycle of hypoxia in the Chester River is characterized by warm-season peaks, where the most spatially and temporally extensive O_2 depletion occurred near the mouth of the estuary (i.e., boundary adjacent to Chesapeake Bay) along the deepest

TABLE 1. Characteristics of stations used in model validation, sediment rate process measurements, and derived metabolic estimates and continuous water properties. Data sources included in the text.

Station Code	System	Latitude	Longitude	Depth, m	Mean salinity	Measurement type	Years visited
CHE0348	Chester River	39.2403	−75.9586	1.7	0.68	Continuous Monitoring; Metabolism Estimates	2003–2006
XIH0077	Chester River	39.1666	−76.0387	3.0	4.69	Continuous Monitoring; Metabolism Estimates	2003–2006
XHH3851	Corsica River	39.0628	−76.0816	1.8	6.88	Continuous Monitoring; Metabolism Estimates	2003–2017
XHH5046	Corsica River	39.0832	−76.1073	1.9	7.81	Continuous Monitoring; Metabolism Estimates	2005–2006
XHH4931	Corsica River	39.0812	−76.1149	2.4	8.44	Continuous Monitoring; Metabolism Estimates	2006–2017
XHH4916	Corsica River	39.0818	−76.1392	4.2	8.73	Continuous Monitoring; Metabolism Estimates	2006–2011
XGG8458	Chester River	38.9734	−76.2367	0.8	10.9	Continuous Monitoring; Metabolism Estimates	2007–2009
XGG8359	Chester River	38.9713	−76.2357	0.6	11.13	Continuous Monitoring; Metabolism Estimates	2007–2009
CR01	Chester River	39.2420	−75.9482	2.8	0.20	Sediment-Water Flux & Sediment Nutrients	2001
CR02	Chester River	39.2391	−76.0080	2.7	1.14	Sediment-Water Flux & Sediment Nutrients	2001
CR06	Chester River	39.1652	−76.0459	2.3	5.40	Sediment-Water Flux & Sediment Nutrients	2001
CRb	Corsica River	39.0786	−76.0979	2.2	8.06	Sediment-Water Flux & Sediment Nutrients	2006
CR08	Chester River	39.1282	−76.0966	7.7	9.23	Sediment-Water Flux & Sediment Nutrients	2001
CR09	Chester River	39.1100	−76.1277	3.5	9.48	Sediment-Water Flux & Sediment Nutrients	2001
CR16	Chester River	39.1031	−76.1421	5.7	9.65	Sediment-Water Flux & Sediment Nutrients	2001
CR19	Chester River	38.9989	−76.2016	6.3	11.68	Sediment-Water Flux & Sediment Nutrients	2001
CR18	Chester River	39.0285	−76.1849	7.3	11.70	Sediment-Water Flux & Sediment Nutrients	2001
XIH4495	Chester River	39.2387	−76.0034	2.6	0.23	Water Column Nutrients, Chl-a, Temp, Salinity	2003
ET4.1	Chester River	39.2437	−75.9249	4.4	0.54	Water Column Nutrients, Chl-a, Temp, Salinity	1984–2019
XIH0077	Chester River	39.1667	−76.0387	3.6	4.89	Water Column Nutrients, Chl-a, Temp, Salinity	2003–2006
XHH7848	Chester River	39.1298	−76.0877	7.3	5.43	Water Column Nutrients, Chl-a, Temp, Salinity	2003
XHH4822	Corsica River	39.0804	−76.1303	4.5	7.02	Water Column Nutrients, Chl-a, Temp, Salinity	2003–2005
XHH6419	Chester River	39.1076	−76.1345	3.8	7.41	Water Column Nutrients, Chl-a, Temp, Salinity	2003–2006
XHG1579	Chester River	39.0257	−76.2017	2.6	8.50	Water Column Nutrients, Chl-a, Temp, Salinity	2003–2006
CB3.2	Chesapeake Bay	39.1637	−76.3063	12.5	9.47	Water Column Nutrients, Chl-a, Temp, Salinity	1984–2019
CB3.3E	Chesapeake Bay	39.0041	−76.3452	8.0	10.08	Water Column Nutrients, Chl-a, Temp, Salinity	1984–2019
ET4.2	Chester River	38.9923	−76.2151	15.0	10.47	Water Column Nutrients, Chl-a, Temp, Salinity	1984–2019

part of the river channel (Figure 1). Deep channel hypoxia dominates the volume of low-O_2 water in the estuary and is highly influenced by exchange with near-anoxic waters at the open-water boundary with the mainstem of the Chesapeake Bay. The results of idealized scenario simulations of (1) warming, (2) nutrient reductions, and (3) exchange of higher oxygen bottom water from the open boundary with the Chesapeake Bay indicate that the extent of low-O_2 water was more sensitive to warming and exchanges with the mainstem Chesapeake Bay bottom water O_2 than it was to reductions in watershed nitrogen and phosphorus inputs.

Water-Column Model Validation

Model simulations reasonably captured the observed seasonal variability in several key properties (i.e., water temperature, salinity, NO_{23}, NH_4, dissolved O_2, and PO_4) in most estuarine regions, but underestimated peak seasonal values for chl-a (ME < 0; Table 2; Figure 4). Dissolved oxygen was well-represented by the model, with RI predominantly <1.3 and a seasonal O_2 cycle that mirrored water temperature, with mid-summer maxima in temperature and minima in bottom O_2 (Figure 4). The RMSE

for NO_{23} was low (generally < 0.5 mg L^{-1}) relative ambient concentrations, whereas NH_4 was typically overestimated by the model (ME > 0; Table 2). NH_4 was elevated during warmer months in both the modeled and observed surface values in the upper and middle reaches of the estuary. In 2003, freshwater discharge into the Chester River was characterized by several 3–4 week periods of elevated flow, with peaks during March, June, and November–December (Figure 3). Consequently, there was not a clear seasonal cycle in modeled or measured nutrient concentrations, outside a winter peak in NO_{23} and PO_4, and modeled PO_4 concentrations were generally lower than those observed (ME < 0, RI ~3). There was a clear spring bloom peak in chl-a in the lower reaches of the estuary, with modeled and observed values reaching peaks between 40 and 60 μg/L (Figure 4), but model-simulated surface chl-a was lower than observed (ME < 0, RI = 2.2; Table 2).

Ecosystem Metabolism Dynamics and Validation

Estimates of P_g (GPP), R_t, and NEM from observed O_2 time series were highly correlated with temperature on a seasonal basis, but the magnitude of rates varied spatially with differences in chlorophyll-a (Figures 5

TABLE 2. Model performance metrics across eight locations in the Chester River estuary, including the root mean square error (RMSE), mean error (ME), and reliability index (RI) for water-column chlorophyll-a, dissolved oxygen (O_2), ammonium, nitrate + nitrite, and phosphate. For ET4.2, "S" is surface water (0.5 m) and "B" is bottom water.

Station	Metric	Chl-a mg L^{-1}	O_2 mg L^{-1}	NH_4 mg L^{-1}	NO_{23} mg L^{-1}	PO_4 mg L^{-1}
XIH4495	RMSE	7.36	1.83	0.11	0.33	0.038
Salinity = 0.2	ME	3.56	1.81	−0.06	0.05	−0.032
Depth = 2.4	RI	3.0	1.3	2.6	1.3	2.8
XIH0077	RMSE	4.81	1.22	0.11	0.73	0.042
Salinity = 3.2	ME	−2.85	0.97	0.06	0.69	−0.039
Depth = 4.8	RI	2.8	1.2	2.0	2.2	3.0
XHH7848	RMSE	10.3	1.54	0.13	0.58	0.023
Salinity = 5.2	ME	−6.22	1.20	0.06	0.55	−0.018
Depth = 4.6	RI	2.4	1.2	2.3	2.6	2.0
XHH6419	RMSE	27.84	1.46	0.14	0.43	0.018
Salinity = 6.4	ME	−16.88	−0.15	0.12	0.39	−0.007
Depth = 3.3	RI	3.5	1.2	5.0	3.2	2.9
XHG1579	RMSE	29.93	2.79	0.09	0.27	0.009
Salinity = 7.6	ME	−15.94	−1.37	0.07	0.23	0.002
Depth = 2.8	RI	2.7	1.3	5.0	4.6	3.0
ET4.2, Surface	RMSE	13.54	1.67	0.11	0.23	0.012
Salinity = 7.8	ME	−6.20	−1.03	0.03	0.15	0.002
Depth = 13.0	RI	2.2	1.2	4.1	2.3	2.9
ET4.2, Bottom	RMSE	14.87	3.45	0.16	0.28	0.015
Salinity = 10.4	ME	−7.05	0.56	0.004	0.19	−0.001
Depth = 13.0	RI	2.9	3.1	3.5	2.5	2.8

and 6). May–October mean values of respiration, for example, ranged from 50 to 250 mmol O_2 m^{-2} d^{-1} (~1.6–8 g O_2 m^{-2} d^{-1}) over the years of record, and were elevated within the sub tributary stations of the Corsica River (The Sill, Sycamore Point, Possum Point, Emory Creek) relative to the two stations in the main body of the Chester (Rolph's Wharf, Deep landing; Figures 2

and 5). Median measured chlorophyll-a concentrations at the Corsica River stations were 13.8–36.3 μg/L, which were 50% higher than chlorophyll-a concentrations measured over a similar period in the adjacent Chester River (6.3–12.5 μg/L; Table S3). Respiration rates at a given temperature were higher under conditions of elevated chlorophyll within stations (Figure 6). For the two stations located within a small inlet in the lower Chester River estuary (Kent Narrows "Inside" and "Outside"; Figure 2), computed respiration rates were a factor of two larger at the inner, more protected station than the outer station (Figure 5). As a consequence, the temperature-respiration slope was 2.5 times higher in the inner station than the outer station (Figure 6). Despite these spatial differences, rates of R_t were significantly correlated with temperature at all sites, but with lower slopes in the main Chester channel region (Figure 6). Regressions of R_t vs. temperature reveal that mean slopes of −8 and −14.1 mmol O_2 m^{-2} d^{-1} °C^{-1} for the Chester River estuary and Corsica River estuary, respectively. Rates of NEM were predominantly negative across all stations in the estuary and NEM was negatively correlated with temperature (i.e., more heterotrophy with higher temperatures) at all but one of the Chester River stations analyzed, with slopes ranging from 0.41 to −1.05 mmol O_2 m^{-2} d^{-1} (Figure S6).

Warming Impacts on Dissolved Oxygen and Metabolic Rates

Warming scenarios with elevated water temperatures of 0.75°C and 1.25°C relative to 2003 conditions
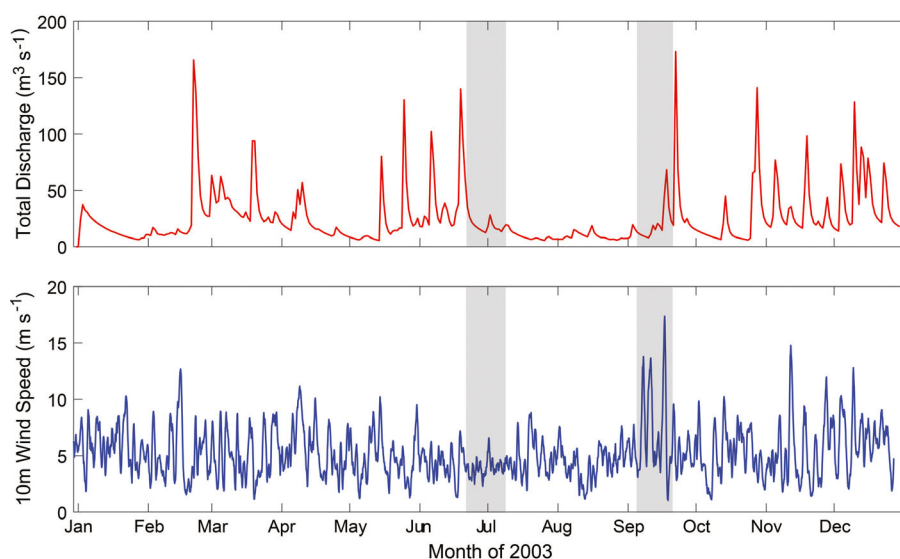

FIGURE 3. Annual hydrograph of total freshwater discharge into the Chester River (top) and local wind speed derived in 2003. Shaded periods in the top and bottom panels highlight two periods where oxygen was depressed below 4 mg L^{-1} at a shallow-water location within the Chester River estuary (see Figure 12).
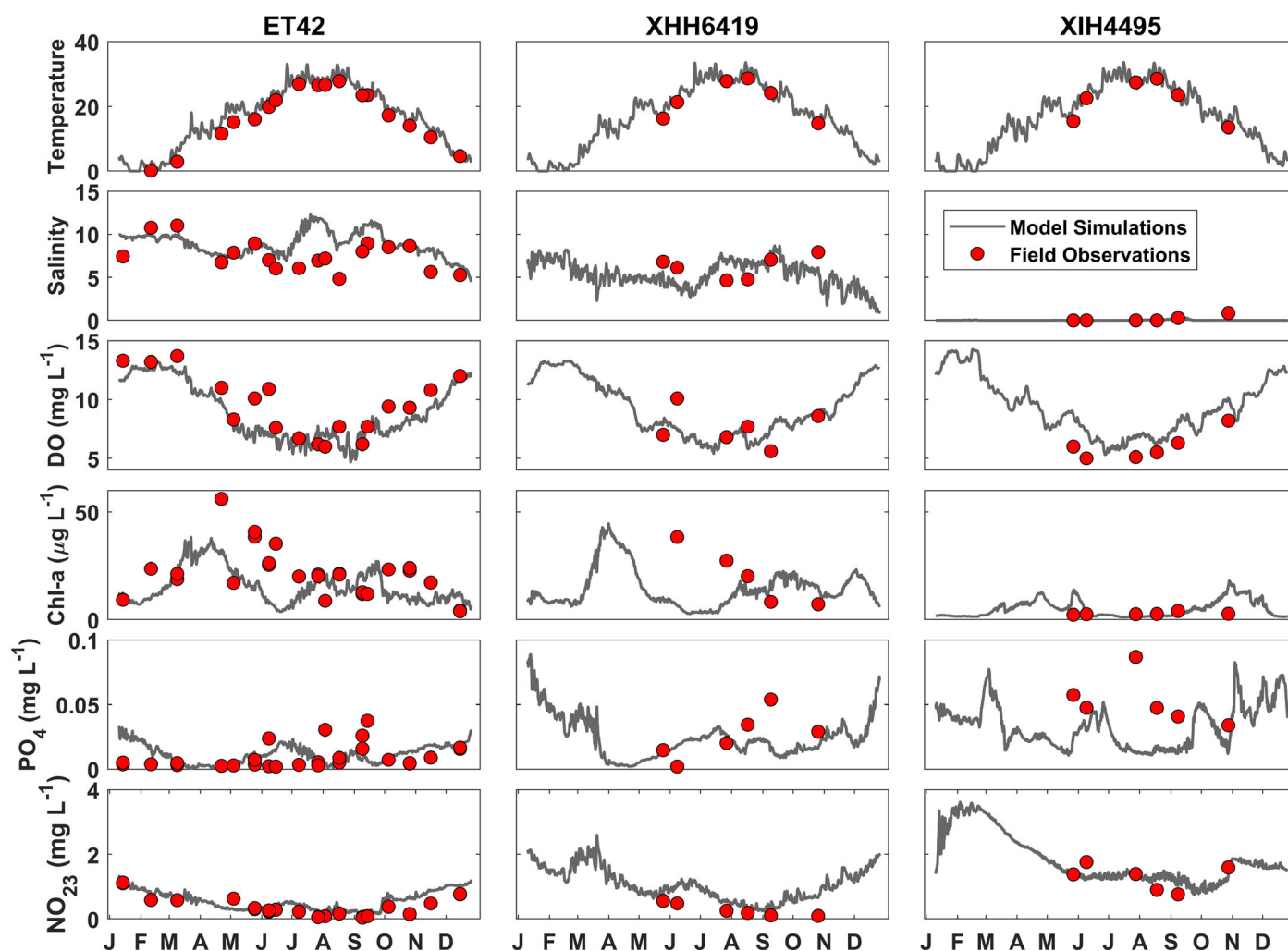
FIGURE 4. Comparisons of model-simulated (lines) and observed (closed circles) surface water properties at three stations oriented along the channel of the Chester River estuary, including water temperature, salinity, DO (O_2), chlorophyll-a, phosphate, and nitrate + nitrite (see Figure 2 for station locations).

predicted lower surface and bottom O_2 concentrations (Figure 7). In both surface and bottom waters, O_2 concentrations were lowered by 0.1–0.2 mg O_2 L^{-1} under a 0.75°C warming and by 0.1–0.8 mg O_2 L^{-1} in the 1.25°C warming scenario (Figure 7). The declines in O_2 in response to warming were highest during the March to August period, except during a period between days 160 and 190 (mid-June to mid-July) where riverine inputs were high (Figure 3) and between days 210 and 225 (early August) where an influx of high O_2 water from mainstem Chesapeake Bay offset O_2 reductions due to warming (Figure 7). Depending on the season, the percentage decrease in O_2 concentrations ranged from 4% during spring and up to 7% during summer under the 1.25°C warming scenario (Figure 7). We also controlled for the impacts of temperature by examining changes in solubility associated with a 1.25°C warming at surface

pressure and a salinity of 7, and found that O_2 declines above 0.3 mg O_2 L^{-1} exceed that expected from solubility changes, which were simulated for spring and late summer periods (Figure 7).

We also quantified changes in estuary-wide volumes of low-O_2 water resulting from warming and considered volumes with O_2 concentrations <5, 3.2, and 2 mg O_2 L^{-1}, which roughly correspond with O_2 criteria used in Chesapeake Bay water quality management (Zhang et al. 2018). The volumes of all low-O_2 waters increased with warming, and the volume expansions per rate of warming (ΔVolume/Δ°C) were similar across the two warming scenarios, as were the relative size of the volume expansion relative to base conditions (5%–7% increase). There were little differences in low O_2 volumes among the scenarios during the August oxygenation event associated with the Chesapeake Bay boundary water influx, except
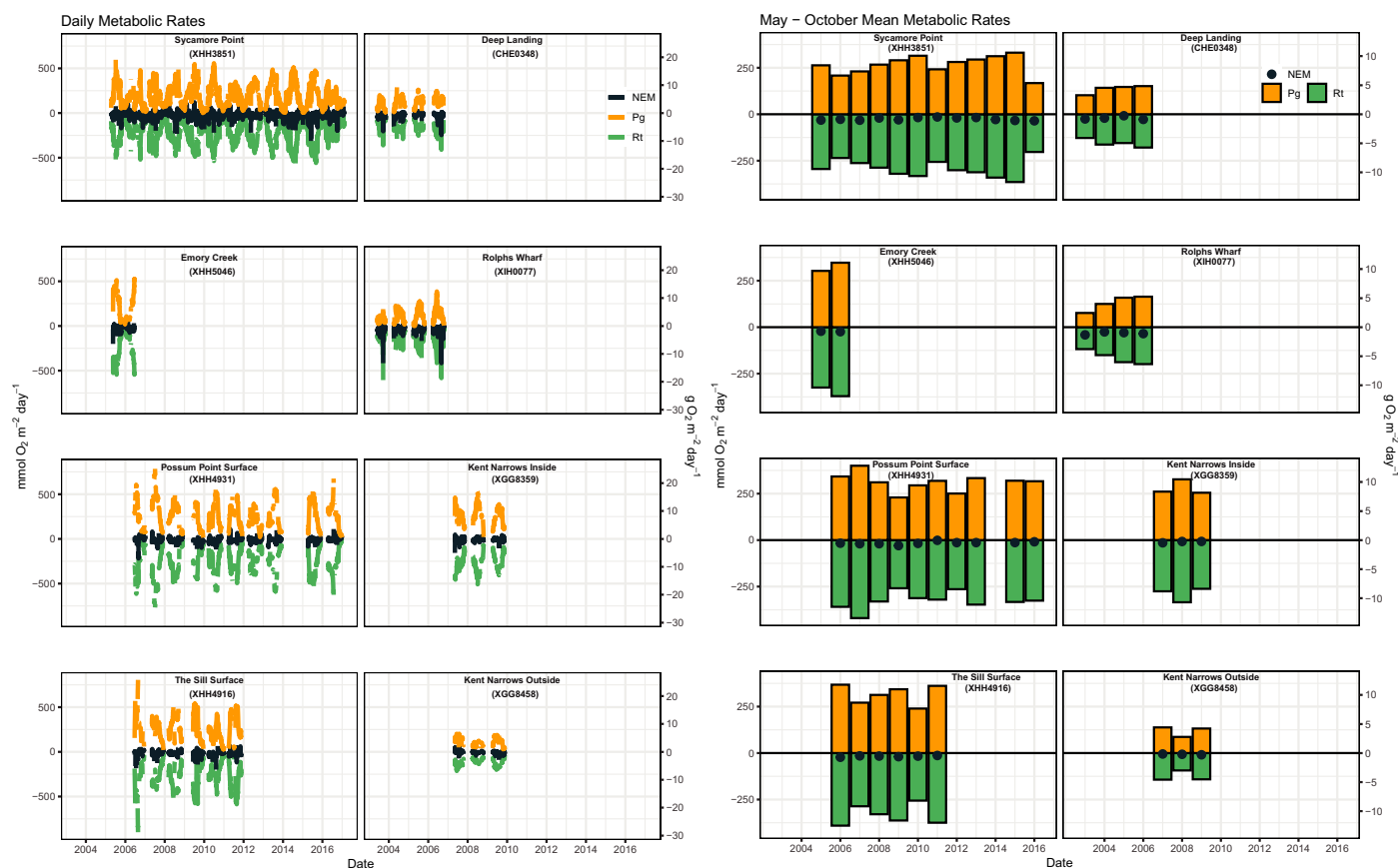
FIGURE 5. Daily (left) and May-October average (right) rates of P_g, R_t, and net ecosystem metabolism (NEM) derived from continuous oxygen time-series across eight stations in the Chester River estuary. Computations made using an approach of Beck et al. (2015). For each time period, the left panels are Corsica River subtributary stations (Sycamore Point, Emory Creek, Possum Point, The Sill) and the right panels are in the main Chester River body (Deep Landing, Rolphs Wharf, Kent Narrows Inside and Outside). Salinity increases from top to bottom (see Figure 2 and Table 1 for station details).

for the 5 mg O_2 L^{-1} threshold where volumes increase by 2%–3% (Figure 8).

Warming also altered ecosystem metabolic rates in the Chester River, leading to increases in NEM during cool seasons and declines in NEM in warm seasons (Figure 9). In the middle region of the estuary (Station XIH0077), warming led to elevated winter-spring GPP (which is equivalent to the observation-based P_g) by 20%–120% during February to March, and reduced GPP during mid-summer (17%–41% decrease from July to September) under 1.25°C warming (Figure 9). Respiration under warming also had a seasonally dependent response, with increases in respiration (1%–14% under 1.25°C warming) in all months except the periods where transitions in phytoplankton groups occurred, including April–May, and September and November (Figure 9). The warm-season respiration amplification and GPP reductions during spring and fall months under warming led to enhancement of net heterotrophic conditions (increasingly negative NEM) in nearly all months of the year, except during February–March (Figure 9). The relative decrease in NEM was proportionally larger than the changes in GPP and respiration under warming, revealing the multiplicative effects of lower GPP and elevated respiration.

Nitrogen and Phosphorus Reduction Scenarios

At the estuary scale, the idealized simulations with 50% reductions in nitrate (NO_{23}) and phosphate (PO_4) loading resulted in only marginal changes in the three thresholds of hypoxic volume (Figure S4), but revealed that P limitation is more important than N limitation. For example, rates of modeled GPP and respiration were reduced by 6%–18% (GPP) and 1%–9% (respiration) during the May–October period in the PO_4 load reduction scenarios and unaffected by changes in NO_{23} loads (Figure 10). Correspondingly, PO_4 reductions caused a decrease in hypoxic volume of 1%–1.5% relative to the Base (no change) scenario,
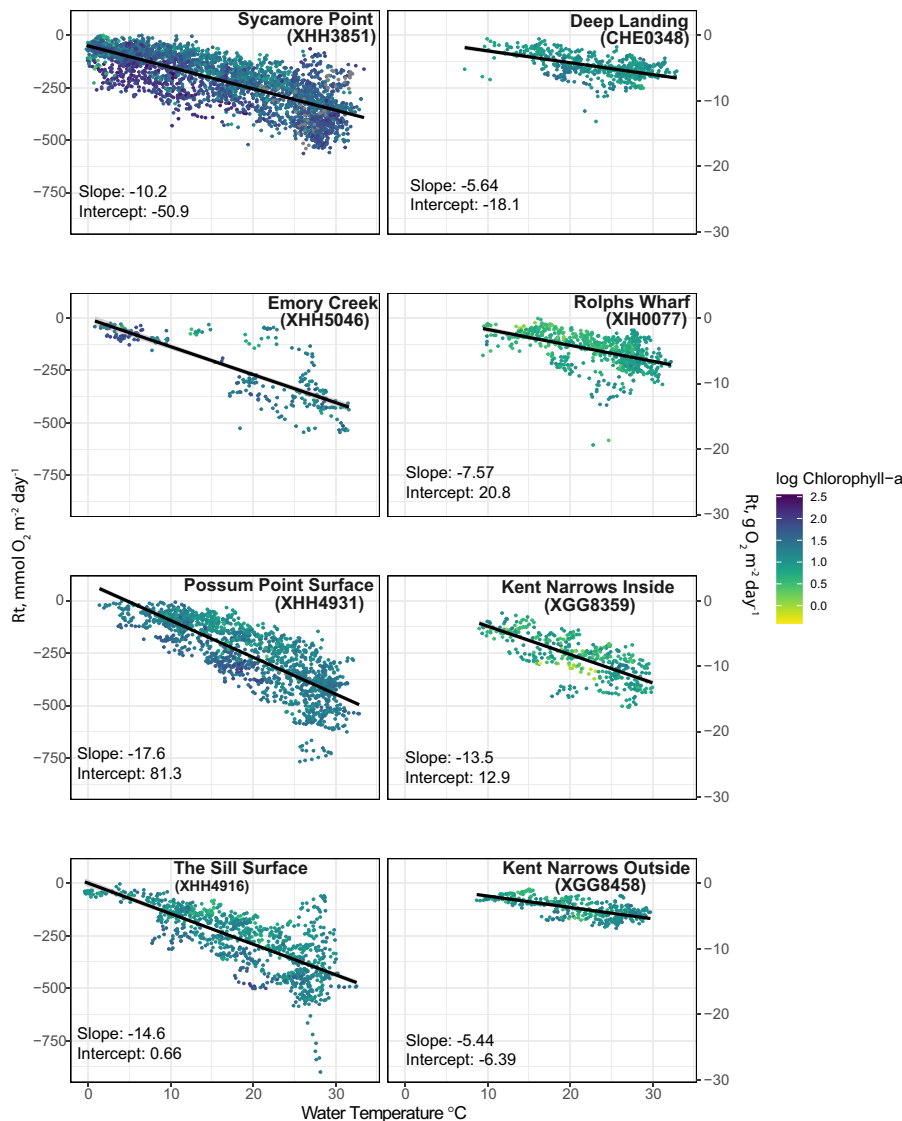
FIGURE 6. Relationships between daily water temperature and daily rates of ecosystem respiration derived from dissolved oxygen time series. The color of circles represents the mean daily log chlorophyll-a. R_t is a rate of oxygen uptake, where increasingly negative values indicate higher respiration. For each regression, the slope and intercept (in units of mmol O_2 m^{-2} d^{-1}) are included. See Figure 2 and Table 1 for station information and location.

with a comparably minor increase in response to NO_{23} reductions.

Dissolved Oxygen at the Chesapeake Bay Boundary Scenario

Scenarios that included elevated O_2 at the Chesapeake Bay boundary had a larger effect on the hypoxic volume within the Chester River than watershed nutrient load reductions or temperature increases. By increasing the O_2 in the subsurface layers of the boundary domain at a level consistent with recently observed "best-case" scenarios in the Chesapeake Bay (year 2001), the total hypoxic volume between June and September decreased by a range of 7%–55% at the threshold of 2 mg O_2 L^{-1}), 4%–40% for the 3.2 mg O_2 L^{-1} threshold, and 4%–30% at the 5 mg O_2 L^{-1} threshold (Figure 11; Table S4). These boundary-exchange effects were largest in absolute terms during late summer hypoxic periods, but were also substantial during the lower volume periods (August, October; Table S4). We did not examine the impacts of sea level changes or examine fine temporal-scale variations associated with tidal mixing.
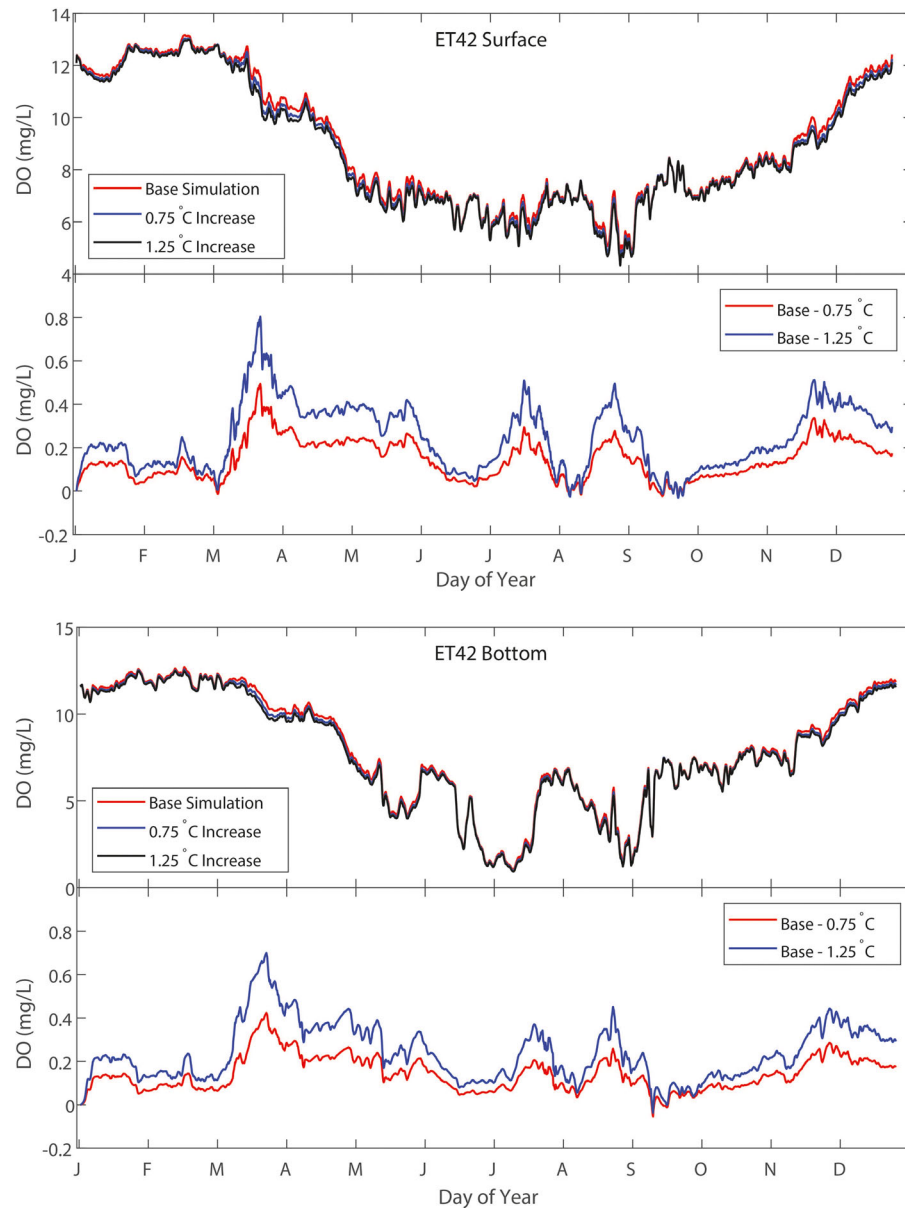
FIGURE 7. Model-simulated dissolved oxygen concentrations and deviations from the baseline simulation under warming (Base-degree increase) in surface (top panels) and bottom waters (bottom panels) in the region of ET4.2 in 2003.

DISCUSSION

We used data-derived estimates of metabolic rates and numerical model simulations of future warming scenarios to examine the sensitivity of a shallow estuarine ecosystem to future warming. Results indicate that warming will elevate respiration rates and associated O_2 consumption, but the magnitude of the temperature-dependency of respiration is positively correlated with local productivity. Warming reduced O_2 concentrations throughout the estuary, with contributions from reduced solubility generally exceeding

those from elevated respiration outside the spring and late-summer periods. This particular estuary, which is turbid and nutrient-rich, was relatively insensitive to relatively large (50%) local watershed nutrient reductions. In contrast, relatively small increases in O_2 in open-water boundary reduced overall hypoxia in the estuary, highlighting the influence of the Chesapeake Bay hypoxia on the Chester River hypoxia and thus the need for watershed-scale nutrient reductions to address local tributary O_2 conditions.

Temperature is a primary driver of ecosystem primary production (GPP, or P_g), respiration (R_t), and NEM based on analyses of recent continuous O_2
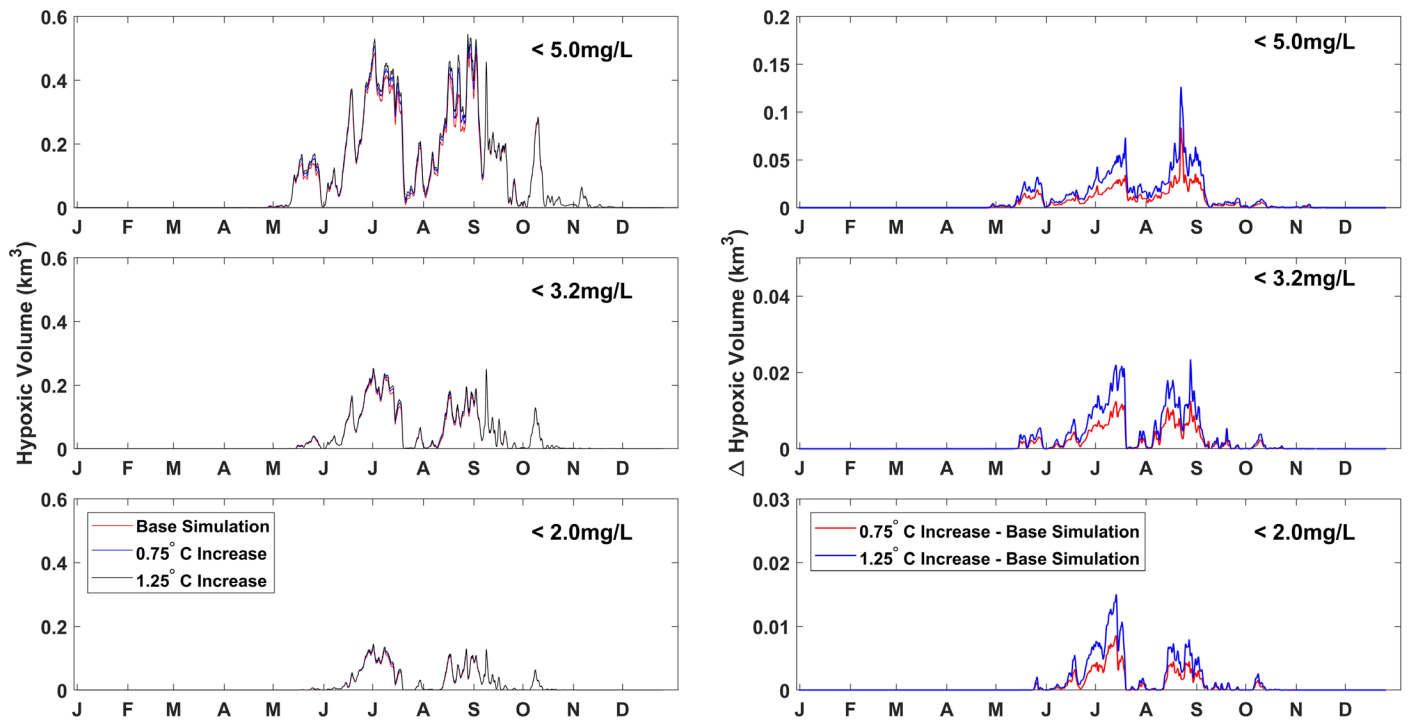
FIGURE 8. Time-series of model-computed volumes of low-oxygen water across the entire Chester River estuary computed below multiple thresholds (<5, 3.2, and 2 mg O_2 L^{-1}) under baseline scenarios and under warming of 0.75°C and 1.25°C (left panels) and differences (Δ Hypoxic Volume) between warming scenarios and the baseline simulation in the Chester River (right panels).
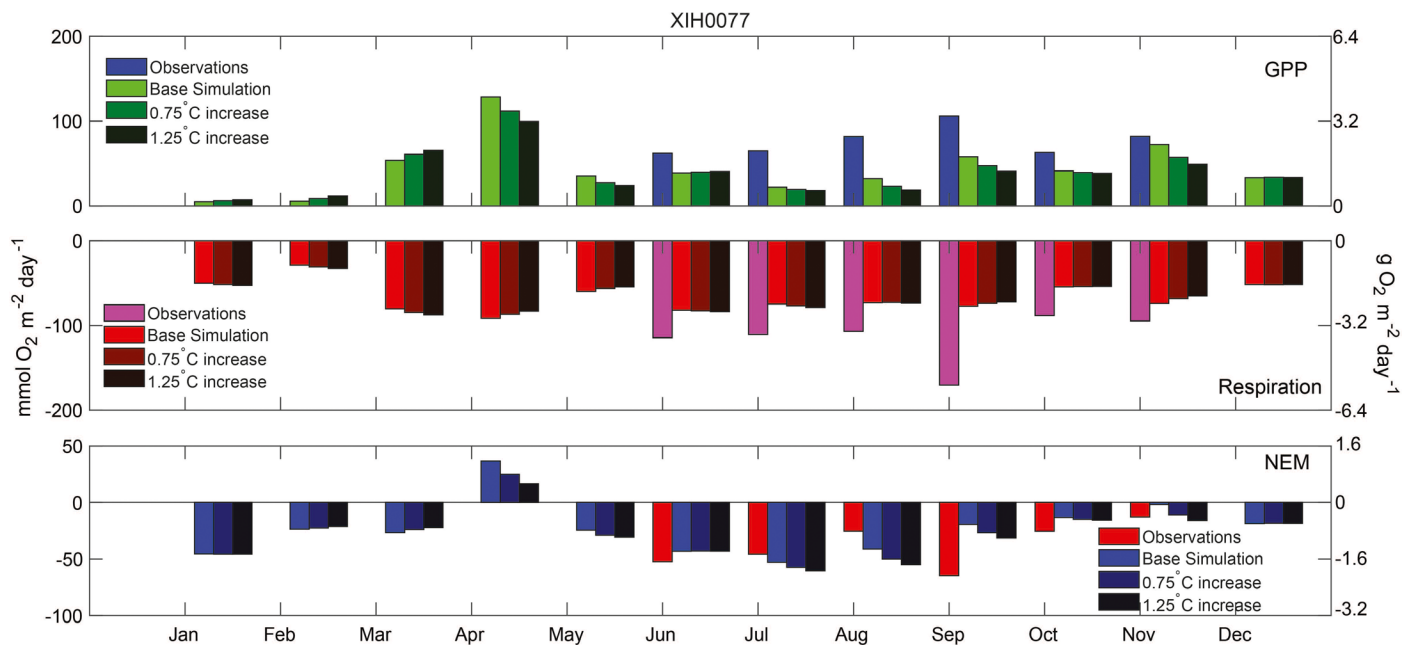

FIGURE 9. Monthly mean modeled and derived rates of water-column and sediment integrated gross primary production (GPP; top panel), respiration (middle panel), and NEM (bottom panel) at station XIH0077 (see Figure 2). Modeled rates include the 2003 simulation and warming simulations with +0.75°C and +1.25°C.

records (2003–2017) and model simulations in the Chester River estuary. Temperature is often cited as a primary driver of metabolic rate processes across

ecosystems (Yvon-Durocher et al. 2012; Caffrey et al. 2014), supporting predictions and assertions that future warming should elevate respiration rates and
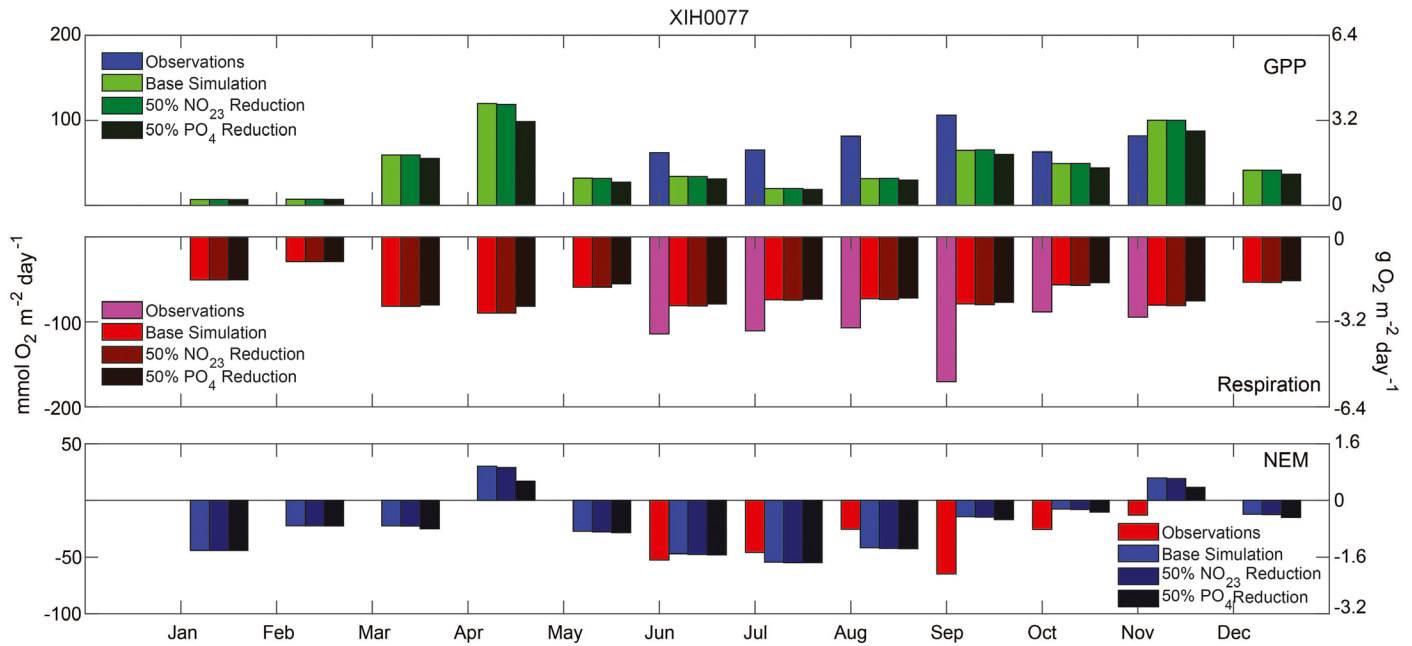
FIGURE 10. Monthly mean modeled and derived rates of water-column and sediment integrated GPP (top panel), respiration (middle panel), and NEM (bottom panel) at station XIH0077 (see Figure 2). Modeled rates include the 2003 simulation and scenarios with a 50% reduction in nitrate (NO$_{23}$) and phosphate (PO$_4$) loading.
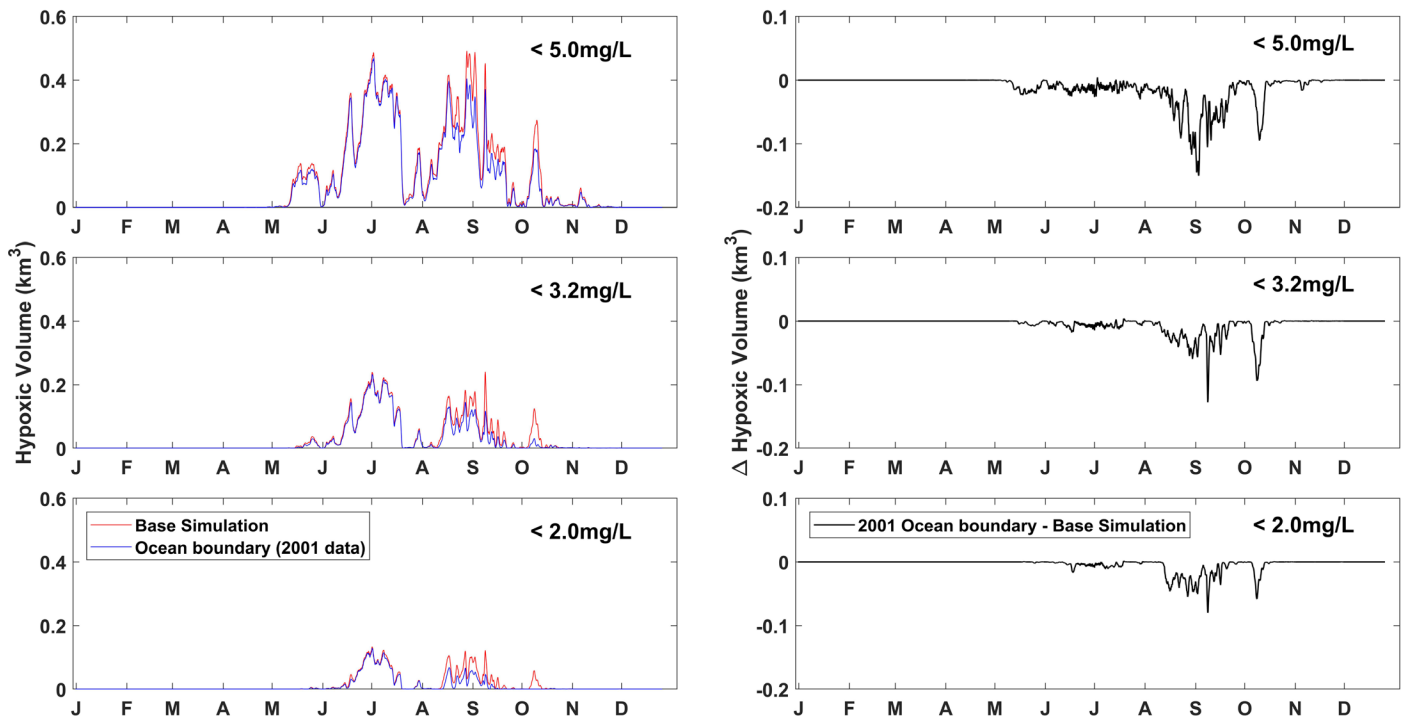

FIGURE 11. Time-series of model-computed volumes of low-oxygen water computed across the entire Chester River estuary below multiple thresholds (< 5, 3.2, and 2 mg O$_2$ L^{-1}) under baseline scenarios and with open-water boundary conditions based on 2001 in the Chesapeake Bay (left panels) and differences (Δ Hypoxic Volume) between the altered boundary scenario and the baseline simulation (right panels) in the Chester River.

O$_2$ depletion (Carstensen et al. 2014; Breitburg et al. 2018; Ni et al. 2019), but the net balance between temperature-effects on GPP and R_t ultimately controls oxygen responses. Observation-derived NEM in the Chester estuary was negatively correlated with temperature (Figure S6), consistent with model

scenarios that suggest future warming will enhance net heterotrophy and further contribute to low O_2 concentrations. This is consistent with predictions of increasing net heterotophy in a warmer future climate, which in part derive from predictions of a higher sensitivity of respiration to temperature than photosynthesis (Yvon-Durocher et al. 2010). However, modeling studies in the other Chesapeake Bay tributaries suggest a more complex picture. For example, Lake and Brush (2015) found that warming increased net primary production (NPP) in upper estuarine regions due to enhanced nutrient remineralization, but reduced NPP in down-estuary regions during summer. Tassone and Bukaveckas (2019) found rates of metabolism in the James River estuary (e.g., median NEM $\sim\pm2$ g O_2 m^{-2} d^{-1}) that were similar to our estimates in the Chester River (Figure S6), but they also reported clear spatial patterns in metabolic rates that might suggest that internal spatial controls on NEM might lead to a varying response of NEM to warming.

NEM responses to warming are complicated by the fact that GPP and R_t tend to be highly correlated, given that organic matter generated by GPP fuels R_t. In the Chester River estuary, the increase in respiration rate in response to warming (e.g., the slope of R_t vs. °C regressions) varied by a factor of three across stations, where the temperature sensitivity of R_t within protected, productive (e.g., high chlorophyll-a, high GPP) waters (slopes = −10.2 to −17.6) was much higher relative to more open, less productive waters (slopes = −5.44 to −7.57). Thus, respiration-derived increases in O_2 consumption in response to future warming will be a function of spatially variable, local productivity and organic matter availability (Testa and Kemp 2008; Lake and Brush 2015). As a consequence, eutrophication abatement and associated productivity declines may allow for increased resilience to warming if associated respiration rates in underlying deep waters or during night are reduced (Irby et al. 2018; Laurent et al. 2018). Our model simulations indicated that GPP declined in response to warming during some seasons (as temperature exceeded optimal phytoplankton growth rates), whereas GPP derived from oxygen time series was positively correlated with temperature, with slopes ranging from 5.13 to 16.5 mmol O_2 m^{-2} d^{-1}. Given the flexible and dynamic nature of phytoplankton communities in response to environmental change, however, such GPP reductions in response to warming may not emerge if species shift to organisms that grow at maximal rates under warming temperatures or if warming-induced nutrient remineralization stimulates additional GPP (e.g., Lake and Brush 2015). Given the complex nature of plankton food web responses to warming (Murphy et al. 2020), the

ability of the simple phytoplankton models used in this analysis to predict future change is limited. Nevertheless, the fact that modeled R_t declined with lower GPP reinforces the strong dependency of these two metabolic indices and their impact on NEM.

The implementation of ROMS-RCA presented here did not include metabolic contributions of benthic primary producers (microalgae, submerged vascular plants; SAV) or exchange with fringing wetland communities, which could have influenced overall metabolic responses to simulated warming. Several prior investigations in the nearby Chesapeake Bay tributaries (York River, James River) have indicated that benthic contributions to ecosystem metabolism can be substantial (Bukaveckas et al. 2011; Qin and Shen 2019). Modeled rates of GPP and respiration were generally lower than those derived from observed oxygen time-series (Figure 9), which may reflect the omission of these important communities. Annual surveys of SAV coverage did not, however, indicate substantial cover of these vascular plants in any region of the Chester River in 2003 (VIMS 2020), suggesting that omission of SAV did not influence model outcomes. Although benthic microalgal communities can be important components of estuarine metabolism in shallow, clear water environments (Miller et al. 1996), typical values of light attenuation in the Chester estuary (mean $k_{dPAR} = 3$ m^{-1}) would only allow 1% of surface light to reach sediments at depths shallower than 1.5 m. Given that much higher light levels would be required to allow photosynthetic rates to substantially impact metabolism, the contributions of benthic microalgae in 2003 were likely to be small. This does not mean that benthic respiration is small in the Chester River, as measured rates of sediment oxygen uptake (~30 mmol O_2 m^{-2} d^{-1} or 0.95 g O_2 m^{-2} d^{-1}) are a substantial portion of ecosystem respiration (Figure 9). Tidal exchange between estuaries and fringing tidal wetlands can also serve to supplement estuarine organic matter stocks to support additional respiration (Cai 2011), but we do not have reliable estimates of tidal wetland exchange in the Chester estuary to assess the potential impact on modeled metabolism of omitting exchanges with tidal marshes. In the York River Estuary, it has been shown that respiration increases with warming given the import of dissolved organic carbon from adjacent habitats (Lake and Brush 2015), suggesting that significant organic matter export could impact metabolic rates in this system.

Warming clearly reduced O_2 concentrations and led to elevated low-O_2 volumes and the magnitude of this response was seasonally specific. Warming of 0.75°C and 1.25°C from current conditions led to elevated low O_2 volumes at all three threshold values by between 5 and 10%, suggesting incremental declines

in O_2 with continued warming. This is consistent with model simulations in the York River estuary (Lake and Brush 2015), who also reported that hypoxia was more sensitive to warming in seaward estuarine regions. Prior projections of future warming effects in the Chesapeake Bay mainstem waters indicated that water temperature was a dominant driver of hypoxic volume, with expected mid-21st Century warming expected to cause 10%–30% increases in low O_2 volumes (Irby et al. 2018; Ni et al. 2019). Hindcast simulations in the Chesapeake Bay (1985 to the present) suggest that contemporary warming has already occurred (~0.8°C –1.5°C) and was a stronger control on O_2 than modest reductions (10%–15%) in nutrient loading (Ni et al. 2020). Warming has also been implicated in expanded low O_2 waters in many estuaries and coastal seas (Justíc et al. 1996; Carstensen et al. 2014; Breitburg et al. 2018; Laurent et al. 2018). Although most of these studies examined changes in the volume of extensive hypoxic zones integrated over long time scales (e.g., decades), our results suggest that the impact of warming varies intra-annually, with more expansive increases under periods of high biological productivity and lower external influence from riverine or seaward boundaries. Our results also indicate that daily minima in O_2 are lower under warming (Figure S3), which could lengthen the daily duration of diel cycling hypoxia in this system and other nearby shallow estuaries (Tyler et al. 2009).

Our idealized model simulations show that while the Chester River O_2 dynamics are sensitive to changes in nutrient inputs, this sensitivity is far less than that of the adjacent mainstem Chesapeake Bay and other coastal water bodies (Laurent et al. 2018; Wang et al. 2018; Irby and Friedrichs 2019). Low sensitivity to nutrient inputs is likely the result of high turbidity within this shallower, well-mixed system. Light attenuation coefficients (k_d) of 2–7 m^{-1} (Figure S2) far exceed those typically observed (<1 m^{-1}) in the mainstem of the Chesapeake Bay (Harding et al. 2015). These conditions imply light limitation for phytoplankton growth that is typical for these turbid, low salinity waters (Fisher et al. 1992). Analysis of modeled light limitation factors in ROMS-RCA (RLGHT), which vary between 0 and 1 and where 1 = no light limitation (Testa et al. 2014), reveal that RLGHT was <0.5 for ~25% of the daytime simulation period at the upstream and mid-Chester stations compared to ~5% at ET4.2, the most downstream station near the Chesapeake Bay mainstem. Thus, phytoplankton potential growth rates would be <50% of maximal rates in surface waters over much of the estuarine body for a substantial portion of the annual cycle. This is consistent with observations of spatial patterns of light availability in the Chester estuary,

where TSS and Secchi depth data indicate more substantially light-limited conditions in upstream regions, where higher TSS (20–25 mg L^{-1}), lower Secchi depths (0.2–0.4 m), and higher k_d (3–5 m^{-1}) were reported relative to the lower estuary with TSS of 5–10 mg L^{-1}, Secchi depth of 0.5–1.2 m, and k_d of 1–3 m^{-1}.

Another important factor leading to low sensitivity to nutrient inputs is the high ambient nutrient concentrations in the Chester River estuary. The Chester River has high dissolved nitrogen and phosphorus concentrations relative to 0.07 mg N L^{-1} and 0.007 mg P L^{-1} (Figure 4), the levels generally considered by local water management targets as concentrations above which phytoplankton growth will not be stimulated by additional nutrient inputs (Zhang et al. 2021). Observed NO_{23} and PO_4 concentrations were typically >0.25 mg N L^{-1} and 0.01 mg P L^{-1} at the Chester River stations (Figure 4), much higher than the half-saturation coefficients in ROMS-RCA (0.01 mg N L^{-1} and 0.001 mg P L^{-1}). The ratio of phosphorus (PO_4), nitrogen ($NO_{23} + NH_4$), and silica concentrations to their respective half-saturation coefficients indicated that at both the upstream and downstream stations, none of the above nutrients were limiting, except for phosphorus during a brief period during winter–spring (i.e., ratios >1, data not shown), during which GPP was reduced by PO_4 load reductions scenarios (Figure 10). Tian (2020) recently reported that nutrient loading was an important factor controlling hypoxia in the Chester River using a multi-year numerical model simulation, but the reported half-saturation coefficients for nitrogen and phosphorus uptake (0.5 mg N L^{-1} and 0.0025 mg P L^{-1}) were much larger than those used in the other Chesapeake water quality models (e.g., 0.007–0.025 mg N L^{-1}) (Testa et al. 2014; Feng et al. 2015; Cerco and Noel 2017). This clearly indicates that modest alterations in nutrient loading rates may be expected to have a much more limited impact on phytoplankton growth and hypoxia than the mainstem Chesapeake Bay and other nutrient-limited estuaries.

Of the local nutrient management scenarios we examined, phosphate (PO_4) loading reduction scenarios had a larger effect on metabolic rates and reductions in hypoxic volume than nitrogen reductions. This is consistent with low-salinity waters (the Chester River estuary mean salinity is <10; Table 1) being more often phosphorus limited (Fisher et al. 1992; Jordan et al. 2008) than more seaward, higher salinity waters. The effect of phosphorus load changes on the Chester River compared to nitrogen is the opposite effect to that observed in the Bay mainstem, where hypoxia is more sensitive to nitrogen loads (Testa et al. 2014). While our analysis revealed

that the Chester River nutrient concentrations are often above those limiting to phytoplankton growth, there are large regions of the Chesapeake Bay vulnerable to nitrogen limitation (Kemp et al. 2005). Complex spatial responses to alterations of phosphorus and nitrogen loading have been reported in other costal systems, where phosphorus declines were linked to lower productivity in low-salinity waters, allowing for more nitrogen transport to support N-limited phytoplankton growth downstream (Laurent and Fennel 2014). Tradeoffs in N vs. P limitation have been linked to spatially dependent long-term changes in phytoplankton biomass in the Neuse River estuary (Paerl et al. 2004), but we did not find a strong change in downstream phytoplankton biomass (or hypoxia) in response to P reductions.

Hypoxia was present seasonally in both deep and shallow waters (i.e., Corsica River), but the volume was dominated by deep water (i.e., >10 m) in the lower estuary. Hypoxic volumes have not been previously reported for the Chester River estuary and unsurprisingly, these simulations suggest that volumes < 2 mg O_2 L^{-1} of 0.1–1 km^3 are an order of magnitude smaller than mainstem Bay hypoxic volumes (2–15 km^3) (Murphy et al. 2011; Irby et al. 2016; Testa et al. 2018). The deeper, stratified waters in the lower Chester River estuary appear to be strongly affected by low-O_2 waters encroaching from the adjacent Chesapeake Bay. In the 2003 simulations, bottom water O_2 concentrations increased and hypoxic volume declined in August during a period where the wind speed was weak (Figure 3; indicating no strong mixing). Simultaneously, O_2 concentrations at stations just outside the lower Chester River increased, indicating that cross-boundary exchange was a key factor driving the Chester River hypoxia. Similarly, sensitivity simulations using boundary conditions with higher bottom O_2 conditions in the Chesapeake Bay (2001) relieved hypoxia in the Chester River estuary by 4%–55% (Table S4). In prior simulations of the Chester estuary, removing hypoxic concentrations completely from the open-water boundary reduced the Chester River hypoxic volume by >90% (Basenback 2019). These results highlight that the main volume of hypoxic water in the Chester River is more sensitive to exchange with the Chesapeake Bay than to local watershed nutrient inputs, and reinforces that larger scale regional improvements in O_2 will be communicated to waters connected to the main stem Chesapeake volume. Furthermore, increases in hypoxia in the mainstem Chesapeake Bay associated with warming (Irby et al. 2018; Ni et al. 2019) would thus be expected to support additional hypoxia in the Chester River estuary given this boundary exchange, and thus our estimates of enhanced the Chester River hypoxia under warming may be conservative.

A key response of shallow, highly productive ecosystems to warming and nutrient load reductions is the alteration of daily extremes in oxygen conditions. Diel-cycling hypoxia and other features of high oxygen variability have been reported in the Corsica River estuary, a small tributary of the Chester River (Boynton et al. 2009), as well as a wide variety of coastal and freshwater ecosystems under conditions of eutrophication (D'Avanzo and Kremer 1994; Tyler et al. 2009), algal blooms (Hitchcock et al. 2014), or dense vegetation cover (Andersen et al. 2017). At a station in the Chester River estuary where 15-min O_2 data were available in 2003, hourly O_2 variations were substantial (hourly standard deviation occasionally >2 mg O_2 L^{-1}; Figure 12) and during two events led to O_2 departures below 4 mg O_2 L^{-1} for several hours. Model-simulated O_2 did capture episodic variations outside the annual seasonal cycle, but the short-term variations (~ hourly) were not as large (~0.1 mg O_2 L^{-1}) as observed (Figure 12). The implication of this underestimation of diel-variability is that modeled metabolic rates were likely lower than observed (Figure 9). However, warming scenarios led to clear downward departures in daily O_2 minima (Figure S3), suggesting that warming will lead to not only reductions in mean O_2 but also increases in the duration of diel-cycling hypoxia. Future work should more fully address what is necessary to simulate diel hypoxia cycling, which may including increasing model spatial resolution to adequately capture the small-scale hydrodynamics and associated residence time needed to allow for O_2 to decline and phytoplankton to reach elevated concentrations (e.g., >100 mg m^{-3}) in the Corsica River estuary. Even the 200-m horizontal resolution used in this model, which is substantially higher than models used for the mainstem of the Chesapeake Bay (Testa et al. 2014; Feng et al. 2015) and other coastal ecosystems (Fennel et al. 2013), was insufficient to capture these key dynamics in the Chester estuary.

Increased model resolution may also be necessary to better capture the biogeochemical dynamics that drive metabolic responses to long-term change. For example, while model-simulated rates of NEM were favorably comparable to estimates derived from dissolved oxygen time-series, model estimates of GPP and respiration appear to be lower than those estimated from observations (Figure 9). Model-simulated chlorophyll-a was consistently lower than observed values in the middle regions of the estuary (ME < 0; Table 2), supporting the idea that overall productivity was higher than simulated in 2003. Model underestimation of productivity does not appear to be linked to insufficient nutrient availability, given that the model reasonably captures dissolved nitrogen and phosphorus dynamics (Figure 3) and the nutrient concentrations are not at limiting levels (as discussed above). Finer resolution (<100 m) hydrodynamic simulations
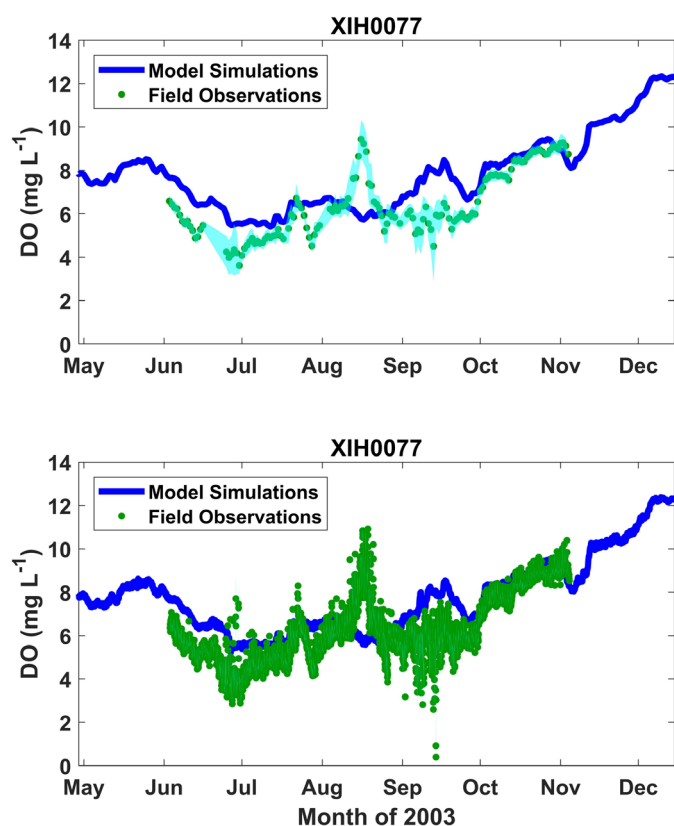
FIGURE 12. Comparisons of modeled (dark blue lines) and observed (green circles) oxygen concentrations (DO) at station XIH0077 (see Figure 2). The top panel includes modeled and observed oxygen values averaged over each 24 h day (where light blue lines are 24-h standard deviation of observations) and the bottom panel is hourly mean modeled and observed oxygen concentrations. Oxygen concentrations at XIH0077 were measured by in situ sensors every 15-min from 1 m below the surface.

have shown a diversity of eddy-like circulation patterns in the Chester River estuary that may locally enhance residence time and allow for more extensive phytoplankton blooms. If we assume that the model did underestimate metabolic rates, our simulated metabolic sensitivity to warming would likely be conservative, and future, higher resolution simulations would allow a test of this hypothesis.

CONCLUSIONS AND FUTURE RECOMMENDATIONS

Our study of O_2 dynamics and metabolic rate processes in response to temperature changes, nutrient load reductions, and boundary conditions reinforces the important role that warming has and will play in regulating water quality dynamics in estuarine ecosystems. Warming will make local management of eutrophic shallow estuaries more difficult due to the

multiple reinforcing ecosystem rates (primary production, respiration, nutrient cycling) that temperature influences. In the Chester River estuary, the role of temperature was particularly relevant because the light-limited and nutrient-saturated nature of the system make it relatively insensitive to changes in watershed nutrient inputs, leading to temperature causing reduced NEM and enhanced heterotrophy. Furthermore, the dominant role of exchange with the mainstem Chesapeake Bay waters in driving the volume of the primary parcel of Chester River hypoxic water demands further analysis of the role of tidal mixing, event scale, and seasonal Chester–Chesapeake interactions. The boundary effect also reveals that long-term changes in connected estuarine systems are inherently linked (Testa et al. 2008) and that the impacts of nutrient reductions and warming on mainstem Chesapeake hypoxia will be communicated to the Chester estuary to enhance or mitigate local warming effects on O_2 concentrations. Despite the fact that the Chester River estuary was relatively insensitive to local nutrient reductions, regional nutrient reductions that improve the mainstem Chesapeake Bay oxygen concentrations will provide benefits to the Chester estuary and other tributary estuaries, whereas local reductions in the Chester River watershed will reduce export through the Chester to the mainstem Bay.

Our results also reinforce that currently established targets for nutrient load reductions aimed at increasing O_2 concentrations may not be sufficient to achieve future oxygen targets given expected warming (Irby et al. 2018; Ni et al. 2019, 2020). Adjustments to these nutrient targets, namely the TMDL, may be necessary to overcome downward-moving targets for O_2 resulting from warming. Emerging technologies have also been proposed to find engineered solutions to low O_2 conditions (Harris et al. 2015; Koweek et al. 2020), but the efficacy of these approaches in larger systems remains unclear (Conley et al. 2009).

While we quantified the impacts of climate warming on the Chester River estuary, warming is only one of several future changes predicted to emerge from global climate changes. In Chesapeake Bay, altered magnitude and seasonality of precipitation and sea level rise are also projected to change, and the hydrodynamic response to these forces will have diverse and interactive impacts on circulation, phytoplankton productivity, and hypoxia (Irby et al. 2018; Ni et al. 2019). Our analysis also focused on a single year (2003, hydrologically moderately wet), thus to test how future warming may impact systems like the Chester River, future work should include more hydrologic variability (i.e., very wet and dry) and specific simulations of altered freshwater inputs that

allow for an understanding of the range of physical variations that could modulate hypoxia responses to warming. This could be especially important in agriculturally dominated watersheds, where climate change will also impact watershed nutrient processing, hydrology, and agriculture conservation practices (Wagena et al. 2018), farmer adaptations to climate change (Huttunen et al. 2015; Chang 2019), and watershed restoration practices that influence sediment load (Palinkas 2013). Ultimately, water quality managers may need to assess optimal strategies in light of sensitivity to warming, changes in hydrological patterns, and tidal boundary conditions, all of which may significantly decrease the efficacy of local watershed management practices.

SUPPORTING INFORMATION

Additional supporting information may be found online under the Supporting Information tab for this article: Included in the Supporting Information is additional statistics on watershed inputs, water properties at the monitoring station, and additional model output and validation analyses.

ACKNOWLEDGMENTS

AUTHORS' CONTRIBUTIONS

Jeremy M. Testa: Conceptualization; data curation; formal analysis; funding acquisition; investigation; methodology; project administration; supervision; validation; visualization; writing-original draft; writing-review & editing. **Nicole Basenback:** Conceptualization; formal analysis; investigation; visualization; writing-original draft; writing-review & editing. **Chunqi Shen:** Data curation; formal analysis; investigation; methodology; validation; visualization; writing-review & editing. **Kelly Cole:** Data curation; formal analysis; investigation; validation; visualization; writing-review & editing. **Amanda Moore:** Data curation; formal analysis; validation; visualization. **Casey Hodgkins:** Data curation; formal analysis; writing-review & editing. **Damian C. Brady:** Conceptualization; funding acquisition; investigation; methodology; project administration; writing-review & editing.

LITERATURE CITED

Altieri, A.H., and K.B. Gedan. 2015. "Climate Change and Dead Zones." *Global Change Biology* 21: 1395–406.

Andersen, M.R., T. Kragh, and K. Sand-Jensen. 2017. "Extreme Diel Dissolved Oxygen and Carbon Cycles in Shallow Vegetated Lakes." *Proceedings of the Royal Society B: Biological Sciences* 284 (1862): 20171427

Basenback, N. 2019. "Phenology of Estuarine Response to Anthropogenic and Climatic Drivers, a Study of the Chesapeake Bay and Chester River Estuaries." Masters thesis, University of Maryland.

Beck, M.W., J.D. Hagy, and M.C. Murrell. 2015. "Improving Estimates of Ecosystem Metabolism by Reducing Effects of Tidal Advection on Dissolved Oxygen Time Series." *Limnology and Oceanography: Methods* 13: 731–45.

Boynton, W.R., M.A.C. Ceballos, E.M. Bailey, C.L.S. Hodgkins, J.L. Humphrey, and J.M. Testa. 2018. "Oxygen and Nutrient Exchanges at the Sediment-Water Interface: A Global Synthesis and Critique of Estuarine and Coastal Data." *Estuaries and Coasts* 41: 301–33.

Boynton, W.R., W.M. Kemp, and C.W. Keefe. 1982. "A Comparative Analysis of Nutrients and Other Factors Influencing Estuarine Phytoplankton Production." In *Estuarine Comparisons*, edited by V.S. Kennedy, 69–90. New York: Academic Press.

Boynton, W.R., J.M. Testa, and W.M. Kemp. 2009. "An Ecological Assessment of the Corsica River Estuary and Watershed Scientific Advice for Future Water Quality Management." In Final Report to Maryland Department of Natural Resource.

Brady, D.C., J.M. Testa, D.M. Di Toro, W.R. Boynton, and W.M. Kemp. 2013. "Sediment Flux Modeling: Calibration and Application for Coastal Systems." *Estuarine, Coastal and Shelf Science* 117: 107–24.

Breitburg, D.L., L.A. Levin, A. Oschlies, M. Grégoire, F.P. Chavez, D.J. Conley, V. Garçon *et al.* 2018. "Declining Oxygen in the Global Ocean and Coastal Waters." *Science* 359 (6371): eaam7240.

Bukaveckas, P.A., L.E. Barry, M.J. Beckwith, V. David, and B. Lederer. 2011. "Factors Determining the Location of the Chlorophyll Maximum and the Fate of Algal Production within the Tidal Freshwater James River." *Estuaries and Coasts* 34: 569–82.

Caffrey, J.M. 2004. "Factors Controlling Net Ecosystem Metabolism in U.S. Estuaries." *Estuaries* 27: 90–101.

Caffrey, J.M., M.C. Murrell, K.S. Amacker, J.W. Harper, S. Phipps, and M.S. Woodrey. 2014. "Seasonal and Inter-Annual Patterns in Primary Production, Respiration, and Net Ecosystem Metabolism in Three Estuaries in the Northeast Gulf of Mexico." *Estuaries and Coasts* 37: 222–41.

Cai, W.-J. 2011. "Estuarine and Coastal Ocean Carbon Paradox: CO_2 Sinks or Sites of Terrestrial Carbon Incineration?" *Annual Review of Marine Science* 3: 123–45.

Carstensen, J., J.H. Andersen, B.G. Gustafsson, and D.J. Conley. 2014. "Deoxygenation of the Baltic Sea during the Last Century." *Proceedings of the National Academy of Sciences of the United States of America* 111: 5628–33.

CBP. 2010. "Chesapeake Bay TMDL Document."

Cerco, C.F., and M.R. Noel. 2013. "Twenty-One-Year Simulation of Chesapeake Bay Water Quality Using the CE-QUAL-ICM Eutrophication Model." *Journal of the American Water Resources Association* 49 (5): 1119–33. https://doi.org/10.1111/jawr.12107.

Cerco, C.F., and M.R. Noel. 2017. "The 2017 Chesapeake Bay Water Quality and Sediment Transport Model." A Report to the U.S. Environmental Protection Agency Chesapeake Bay Program.

Chang, S. 2019. "Effects of Seasonal and Long-term Climate Variability on Nitrate Export in the Chesterville Branch Catchment of the Eastern Shore, MD". Masters Thesis. Baltimore, MD: Johns Hopkins University.

Conley, D.J., E. Bonsdorff, J. Carstensen, G. Destouni, B.G. Gustafsson, L.A. Hansson, N.N. Rabalais, M. Voss, and L. Zillén. 2009. "Tackling Hypoxia in the Baltic Sea: Is Engineering a Solution?" *Environmental Science & Technology* 43: 3407–11.

D'Avanzo, C., and J.N. Kremer. 1994. "Diel Oxygen Dynamics and Anoxic Events in an Eutrophic Estuary of Waquoit Bay, Massachusetts." *Estuaries* 17: 131–9.

Di Toro, D.M. 2001. *Sediment Flux Modeling*. New York: Wiley-Interscience.

Ding, H., and A.J. Elmore. 2015. "Spatio-Temporal Patterns in Water Surface Temperature from Landsat Time Series Data in the Chesapeake Bay, USA." *Remote Sensing of Environment* 168: 335–48.

Feng, Y., M.A.M. Friedrichs, J. Wilkin, H. Tian, Q. Yang, E.E. Hofmann, J.D. Wiggert, and R.R. Hood. 2015. "Chesapeake Bay Nitrogen Fluxes Derived from a Land-Estuarine Ocean Biogeochemical Modeling System: Model Description, Evaluation, and Nitrogen Budgets." *Journal of Geophysical Research: Biogeosciences* 120: 1666–95.

Fennel, K., J. Hu, A. Laurent, M. Marta-Almeida, and R. Hetland. 2013. "Sensitivity of Hypoxia Predictions for the Northern Gulf of Mexico to Sediment Oxygen Consumption and Model Nesting." *Journal of Geophysical Research: Oceans* 118 (2): 990–1002.

Fennel, K., and J.M. Testa. 2019. "Biogeochemical Controls on Coastal Hypoxia." *Annual Review of Marine Science* 11: 105–30.

Fisher, T.R., E.R. Peele, J.W. Ammerman, and J.L.W. Harding. 1992. "Nutrient Limitation of Phytoplankton in Chesapeake Bay." *Marine Ecology Progress Series* 82: 51–63.

Fitzpatrick, J.J. 2009. "Assessing Skill of Estuarine and Coastal Eutrophication Models for Water Quality Managers." *Journal of Marine Systems* 76: 195–211.

Frank, J.M., F.M. Rohland, R.M. Stankelis, J.M. Lawrence, B. Bean, H. Pine, and W.R. Boynton. 2002. "Monitoring of Sediment Oxygen and Nutrient Exchanges in the Chester River Estuary in Support of TMDL Development." Report to the Maryland Department of the Environment, p. 80.

Ganju, N.K., J.M. Testa, S.E. Suttles, and A.L. Aretxabaleta. 2020. "Spatiotemporal Variability of Light Attenuation and Net Ecosystem Metabolism in a Back-Barrier Estuary." *Ocean Science* 16(3): 593–614.

Grantham, B.A., F. Chan, K.J. Nielsen, D.S. Fox, J.A. Barth, A. Huyer, J. Lubchenco, and B.A. Menge. 2004. "Upwelling-Driven Nearshore Hypoxia Signals Ecosystem and Oceanographic Changes in the Northeast Pacific." *Nature* 429: 749–54.

Harding, L.W., C.L. Gallegos, E.S. Perry, W.D. Miller, J.E. Adolf, M.E. Mallonee, and H.W. Paerl. 2015. "Long-Term Trends of Nutrients and Phytoplankton in Chesapeake Bay." *Estuaries and Coasts* 39: 664–81.

Harris, L.A., C.L.S. Hodgkins, M.C. Day, D. Austin, J.M. Testa, W. Boynton, L. Van Der Tak, and N.W. Chen. 2015. "Optimizing Recovery of Eutrophic Estuaries: Impact of Destratification and Re-Aeration on Nutrient and Dissolved Oxygen Dynamics." *Ecological Engineering* 75: 470–83.

Hitchcock, G.L., G. Kirkpatrick, P.V.Z. Lane, and C.J. Langdon. 2014. "Comparative Diel Oxygen Cycles Preceding and during a Karenia Bloom in Sarasota Bay, Florida, USA." *Harmful Algae* 38: 95–100.

Huttunen I., H. Lehtonen, M. Huttunen, V. Piirainen, M. Korppoo, N. Veijalainen, M. Viitasalo, B. Vehviläinen. 2015. "Effects of Climate Change and Agricultural Adaptation on Nutrient Loading from Finnish Catchments to the Baltic Sea." *Science of The Total Environment* 529: 168 –81. https://doi.org/10.1016/j.scitotenv.2015.05.055.

Irby, I.D., M.A.M. Friedrichs, C.T. Friedrichs, A.J. Bever, R.R. Hood, L.W.J. Lanerolle, M. Li *et al.* 2016. "Challenges Associated with Modeling Low-Oxygen Waters in Chesapeake Bay: A Multiple Model Comparison." *Biogeosciences* 13: 2011–28.

Irby, I.D., M.A.M. Friedrichs, F. Da, and K.E. Hinson. 2018. "The Competing Impacts of Climate Change and Nutrient Reductions on Dissolved Oxygen in Chesapeake Bay." *Biogeosciences* 15: 2649–68.

Irby, I.D., and M.A.M. Friedrichs. 2019. "Evaluating Confidence in the Impact of Regulatory Nutrient Reduction on Chesapeake Bay Water Quality." *Estuaries and Coasts* 42: 16–32.

Jordan, T.E., J.C. Cornwell, W.R. Boynton, and J.T. Anderson. 2008. "Changes in Phosphorus Biogeochemistry along an Estuarine Salinity Gradient: The Iron Conveyor Belt." *Limnology and Oceanography* 53: 172–84.

Justíc, D., N.N. Rabalais, and R.E. Turner. 1996. "Effects of Climate Change on Hypoxia in Coastal Waters: A Doubled CO_2 Scenario for the Northern Gulf of Mexico." *Limnology and Oceanography* 41: 992–1003.

Justíc, D., R.E. Turner, and N.N. Rabalais. 2003. "Climatic Influences on Riverine Nitrate Flux: Implications for Coastal Marine Eutrophication and Hypoxia." *Estuaries* 26: 1–11.

Kemp, W.M., W.R. Boynton, J.E. Adolf, D.F. Boesch, W.C. Boicourt, G. Brush, J.C. Cornwell *et al*. 2005. "Eutrophication of Chesapeake Bay: Historical Trends and Ecological Interactions." *Marine Ecology Progress Series* 303: 1–29.

Koweek, D.A., C. García-Sánchez, P.G. Brodrick, P. Gassett, and K. Caldeira. 2020. "Evaluating Hypoxia Alleviation through Induced Downwelling." *Science of the Total Environment* 719: 137334.

Lajaunie-Salla, K., A. Sottolichio, S. Schmidt, X. Litrico, G. Binet, and G. Abril. 2018. "Future Intensification of Summer Hypoxia in the Tidal Garonne River (SW France) Simulated by a Coupled Hydro Sedimentary-Biogeochemical Model." *Environmental Science and Pollution Research* 25: 31957–70.

Lake, S.J. and M.J. Brush. 2015. "Modeling Estuarine Response to Load Reductions in a Warmer Climate: The York River Estuary, Virginia, USA." *Marine Ecology Progress Series* 538: 81–98.

Laurent, A., and K. Fennel. 2014. "Simulated Reduction of Hypoxia in the Northern Gulf of Mexico Due to Phosphorus Limitation." *Elementa: Science of the Anthropocene* 2. https://doi.org/10.12952/journal.elementa.000022.

Laurent, A., K. Fennel, D.S. Ko, and J. Lehrter. 2018. "Climate Change Projected to Exacerbate Impacts of Coastal Eutrophication in the Northern Gulf of Mexico." *Journal of Geophysical Research: Oceans* 123: 3408–26.

Lefcheck, J.S., D.J. Wilcox, R.R. Murphy, S.R. Marion, and R.J. Orth. 2017. "Multiple Stressors Threaten the Imperiled Coastal Foundation Species Eelgrass (*Zostera marina*) in Chesapeake Bay, USA." *Global Change Biology* 23: 3474–83.

Li, M., Y.-J. Lee, J.M. Testa, Y. Li, W. Ni, W.M. Kemp, and D.M.D. Toro. 2016. "What Drives Interannual Variability of Estuarine Hypoxia: Climate Forcing versus Nutrient Loading?" *Geophysical Research Letters* 43: 2127–34.

McGlathery, K.J., K. Sundbäck, and I.C. Anderson. 2007. "Eutrophication in Shallow Coastal Bays and Lagoons: The Role of Plants in the Coastal Filter." *Marine Ecology Progress Series* 348: 1–18.

Meier, H.E.M., H.C. Andersson, K. Eilola, B.G. Gustafsson, I. Kuznetsov, B. Müller-Karulis, T. Neumann, and O.P. Savchuk. 2011. "Hypoxia in Future Climates: A Model Ensemble Study for the Baltic Sea." *Geophysical Research Letters* 38: L24608. https://doi.org/10.1029/2011GL049929.

Miller, D.C., R.J. Geider, and H.L. MacIntyre. 1996. "Microphytobenthos: The Ecological Role of the "Secret Garden" of Unvegetated, Shallow-Water Marine Habitats. II. Role in Sediment Stability and Shallow-Water Food Webs." *Estuaries* 19: 202–12.

Murphy, G.E.P., T.N. Romanuk, and B. Worm. 2020. "Cascading Effects of Climate Change on Plankton Community Structure." *Ecology and Evolution* 10: 2170–81.

Murphy, R.R., W.M. Kemp, and W.P. Ball. 2011. "Long-Term Trends in Chesapeake Bay Seasonal Hypoxia, Stratification, and Nutrient Loading." *Estuaries and Coasts* 34: 1293–309.

Murrell, M.C., J.M. Caffrey, D.T. Marcovich, M.W. Beck, B.M. Jarvis, and J.D.I. Hagy. 2018. "Seasonal Oxygen Dynamics in a Warm Temperate Estuary: Effects of Hydrologic Variability on Measurements of Primary Production, Respiration, and Net Metabolism." *Estuaries and Coasts* 41: 690–707.

Neff, R., H. Chang, C.G. Knight, R. Najjar, B. Yarnal, and H. Walker. 2000. "Impact of Climate Variation and Change on Mid-Atlantic Region Hydrology and Water Resources." *Climate Research* 14: 207–18.

Ni, W., M. Li, A.C. Ross, and R.G. Najjar. 2019. "Large Projected Decline in Dissolved Oxygen in a Eutrophic Estuary Due to Climate Change." *Journal of Geophysical Research: Oceans* 124: 8271–89.

Ni, W., M. Li, and J.M. Testa. 2020. "Discerning Effects of Warming, Sea Level Rise and Nutrient Management on Long-Term Hypoxia Trends in Chesapeake Bay." *Science of the Total Environment* 737: 139717.

Nixon, S.W., R.W. Fulweiler, B.A. Buckley, S.L. Granger, B.L. Nowicki, and K.M. Henry. 2009. "The Impact of Changing Climate on Phenology, Productivity, and Benthic-Pelagic Coupling in Narragansett Bay." *Estuarine, Coastal and Shelf Science* 82: 1–18.

Odum, H.T., and C.M. Hoskin. 1958. "Comparative Studies of the Metabolism of Marine Waters." *Publications of the Institute of Marine Science-University of Texas* 5: 16–46.

Ortiz-Bobea, A., H. Wang, C.M. Carrillo, and T.R. Ault. 2019. "Unpacking the Climatic Drivers of US Agricultural Yields." *Environmental Research Letters* 14: 064003.

Paerl, H.W., L.M. Valdes, A.R. Joyner, and M.F. Piehler. 2004. "Solving Problems Resulting from Solutions: Evolution of a Dual Nutrient Management Strategy for the Eutrophying Neuse River Estuary, North Carolina." *Environmental Science and Technology* 38: 3068–73.

Palinkas, C.M. 2013. "Seasonal and Interannual Patterns of Sedimentation in the Corsica River (MD): Evaluating the Potential Influence of Watershed Restoration." *Estuarine, Coastal and Shelf Science* 127: 37–45, https://doi.org/10.1016/j.ecss.2013.04.015

Qin, Q., and J. Shen. 2019. "Pelagic Contribution to Gross Primary Production Dynamics in Shallow Areas of York River, VA, U.S.A." *Limnology and Oceanography* 64: 1484–99.

Sanford L.P., Boicourt W.C. 1990. "Wind-forced salt intrusion into a tributary estuary." *Journal of Geophysical Research* 95: 13357 .

Shen, C., J.M. Testa, M. Li, W.-J. Cai, G.G. Waldbusser, W. Ni, W.M. Kemp *et al*. 2019. "Controls on Carbonate System Dynamics in a Coastal Plain Estuary: A Modeling Study." *Journal of Geophysical Research: Biogeosciences* 124 (1): 61–78.

Shen, C., J.M. Testa, W. Ni, W.-J. Cai, M. Li, and W.M. Kemp. 2019. "Ecosystem Metabolism and Carbon Balance in Chesapeake Bay: A 30-Year Analysis Using a Coupled Hydrodynamic-Biogeochemical Model." *Journal of Geophysical Research: Oceans* 124: 6141–53.

Shenk, G.W., J. Wu, and L.C. Linker. 2012. "Enhanced HSPF Model Structure for Chesapeake Bay Watershed Simulation." *Journal of Environmental Engineering* 138: 949–57.

Smith, S.V., J.T. Hollibaugh, S.J. Dollar, and S. Vink. 1991. "Tomales Bay Metabolism C-N-P Stoichiometry and Ecosystem Heterotrophy at the Land-Sea Interface." *Estuarine, Coastal and Shelf Science* 33: 223–57.

Stow, C.A., J. Jolliff, D.J. McGillicuddy, S.C. Doney, J.I. Allen, M.A.M. Friedrichs, K.A. Rose, and P. Wallhead. 2009. "Skill Assessment for Coupled Biological/Physical Models of Marine Systems." *Journal of Marine Systems* 76: 12.

Tassone, S.J., and P.A. Bukaveckas. 2019. "Seasonal, Interannual, and Longitudinal Patterns in Estuarine Metabolism Derived from Diel Oxygen Data Using Multiple Computational Approaches." *Estuaries and Coasts* 42: 1032–51.

Testa, J.M., D.C. Brady, D.M. Di Toro, W.R. Boynton, J.C. Cornwell, and W.M. Kemp. 2013. "Sediment Flux Modeling: Nitrogen, Phosphorus and SILICA CYCLES." *Estuarine, Coastal and Shelf Science* 131: 245–63.

Testa, J.M., and W.M. Kemp. 2008. "Variability of Biogeochemical Processes and Physical Transport in a Partially Stratified Estuary: A Box-Modeling Analysis." *Marine Ecology Progress Series* 356: 63–79.

Testa, J.M., W.M. Kemp, W.R. Boynton, and J.D. Hagy. 2008. "Long-Term Changes in Water Quality and Productivity in the Patuxent River Estuary: 1985 to 2003." *Estuaries and Coasts* 31: 1021–37.

Testa, J.M., and W.M. Kemp. 2014. "Spatial and Temporal Patterns in Winter-Spring Oxygen Depletion in Chesapeake Bay Bottom Waters." *Estuaries and Coasts* 37: 1432–48.

Testa, J.M., Y. Li, Y.J. Lee, M. Li, D.C. Brady, D.M.D. Toro, and W.M. Kemp. 2014. "Quantifying the Effects of Nutrient Loading on Dissolved O_2 Cycling and Hypoxia in Chesapeake Bay Using a Coupled Hydrodynamic-Biogeochemical Model." *Journal of Marine Systems* 139: 139–58.

Testa, J.M., R.R. Murphy, D.C. Brady, and W.M. Kemp. 2018. "Nutrient- and Climate-Induced Shifts in the Phenology of Linked Biogeochemical Cycles in a Temperate Estuary." *Frontiers in Marine Science* 5. https://doi.org/10.3389/fmars.2018.00114.

Thébault, J., T.S. Schraga, J.E. Cloern, and E.G. Dunlavey. 2008. "Primary Production and Carrying Capacity of Former Salt Ponds after Reconnection to San Francisco Bay." *Wetlands* 28: 841–51.

Tian, R. 2020. "Factors Controlling Hypoxia Occurrence in Estuaries, Chester River, Chesapeake Bay." *Water* 12 (7): 1961. https://doi.org/10.3390/w12071961.

Tyler, R.M., D.C. Brady, and T. Targett. 2009. "Temporal and Spatial Dynamics of Diel-Cycling Hypoxia in Estuarine Tributaries." *Estuaries and Coasts* 32: 123–45.

VIMS. 2020. *SAV Monitoring & Restoration; Seagrass Area by Segment*. Gloucester Point, VA: Virginia Institute of Marine Sciences.

Wagena, M.B., A.S. Collick, A.C. Ross, R.G. Najjar, B. Rau, A.R. Sommerlot, D.R. Fuka, P.J.A. Kleinman, and Z.M. Easton. 2018. "Impact of Climate Change and Climate Anomalies on Hydrologic and Biogeochemical Processes in an Agricultural

Catchment of the Chesapeake Bay Watershed, USA." *Science of the Total Environment* 637–638: 1443–54.

Wang, B., J. Hu, S. Li, L. Yu, and J. Huang. 2018. "Impacts of Anthropogenic Inputs on Hypoxia and Oxygen Dynamics in the Pearl River Estuary." *Biogeosciences* 15: 6105–25.

Yvon-Durocher, G., J.M. Caffrey, A. Cescatti, M. Dossena, P. del Giorgio, J.M. Gasol, J.M. Montoya, J. Pumpanen, P.A. Staehr, and M. Trimmer. 2012. "Reconciling the Temperature Dependence of Respiration across Timescales and Ecosystem Types." *Nature* 487: 472.

Yvon-Durocher, G., J.I. Jones, M. Trimmer, G. Woodward, and J.M. Montoya. 2010. "Warming Alters the Metabolic Balance of Ecosystems." *Philosophical Transactions of the Royal Society B: Biological Sciences* 365: 2117–26.

Zhang Q., T.R. Fisher, E. M. Trentacoste, C. Buchanan, A.B. Gustafson, R. Karrh, R.R. Murphy, J. Keisman, C. Wu, R. Tian, J.M. Testa, P.J. Tango. 2021. "Nutrient Limitation of Phytoplankton in Chesapeake Bay: Development of an Empirical Approach for Water-quality Management." *Water Research* 188: 116407 http://dx.doi.org/10.1016/j.watres.2020.116407.

Zhang, Q., P.J. Tango, R.R. Murphy, M.K. Forsyth, R. Tian, J. Keisman, and E.M. Trentacoste. 2018. "Chesapeake Bay Dissolved Oxygen Criterion Attainment Deficit: Three Decades of Temporal and Spatial Patterns." *Frontiers in Marine Science* 5. https://doi.org/10.3389/fmars.2018.00422.